AD-787 852

IR WINDOW STUDIES

Ferdinand A. Kroger, et al

University of Southern California

Prepared for:

Defense Advanced Research Projects Agency
Air Force Cambridge Research Laboratories

15 March 1974

UNCLASSIFIED

Security Classification

AD-787852

DOCUMENT CONTROL DATA - R & D

(Security classification of title, body of abstract and indexing annotation must be entered when the overall report is classified)

1 ORIGINATING ACTIVITY (Corporate author) University of Southern California Electronic Sciences Laboratory Los Angeles, California 90007	2a. REPORT SECURITY CLASSIFICATION UNCLASSIFIED 2b. GROUP

3 REPORT TITLE

IR WINDOW STUDIES

4 DESCRIPTIVE NOTES (Type of report and inclusive dates)

Scientific Interim.

5 AUTHOR(S) (First name, middle initial, last name)

Ferdinand Kroger
John H. Marburger

6 REPORT DATE	7a. TOTAL NO. OF PAGES	7b. NO. OF REFS
15 MARCH 1974	67	27

8a. CONTRACT OR GRANT NO	9a. ORIGINATOR'S REPORT NUMBER(S)
F19628-72-C-0275 b. PROJECT ~~XX~~ Task, Work Unit Nos. 2055 n/a n/a c. DoD Element 61101D d. DoD Subelement n/a	Quarterly Technical Report No. 7 9b. OTHER REPORT NO(S) (Any other numbers that may be assigned this report) AFCRL-TR-74-0060

10. DISTRIBUTION STATEMENT

A--Approved for public release; distribution unlimited

11. SUPPLEMENTARY NOTES	12. SPONSORING MILITARY ACTIVITY
This research was supported by the Defense Advanced Research Projects Agency.	Air Force Cambridge Research Laboratories (LQ) L. G. Hanscom Field Bedford, Mass. 01730

13 ABSTRACT

Meltgrown GaAs invariably has the same IR absorption spectrum with $k_{10.6} = 0.008 cm^{-1}$. Annealing at 400°C does not change this absorption. The yield strength of GaAs is increased by formation of $(Si_{Ga} V_{Ga})$ pairs. An apparatus for the growth of GaAs from liquid gallium is almost ready for operation.

The infrared absorption of CdTe doped with 5×10^{16} Cl is practically entirely due to free carriers. For electrons as well as holes, k ∝ concentration. Lowest absorption is found for samples quenched after annealing at 700°C at $P_{Cd} = 5 \times 10^{-2}$ atm.

Cd or Te as liquid sintering aids for CdTe are ineffective because of lack of wetting The capacitance of insulating CdTe is independent of field and frequency from $1\text{-}10^4$V/cm and 10kHz to 1 MHZ. Bromate ions increase the 10.6μm absorption of KBr. A CO_2, TEA laser for damage studies is being tested. Theories have been developed for a non-linear moment contribution to multi-phonon absorption of crystals with NaCl structure; for interaction of surface waves with heated surface; and thermal lensing, including residual birefringence.

i

DD FORM 1 NOV 68 1473 (PAGE 1)

0102-014-6600

UNCLASSIFIED

Security Classification

14 KEY WORDS	LINK A		LINK B		LINK C	
	ROLE	WT	ROLE	WT	ROLE	WT
IR Windows						
Alkali Halides						
III-V Semiconductors						
II-VI Semiconductors						
Thermal Lensing						
IR Absorption						

AFCRL-TR-74-0263

IR WINDOW STUDIES

Ferdinand A. Kroger
John H. Marburger

Electronic Sciences Laboratory
University of Southern California
Los Angeles, California 90007

15 March 1974

Quarterly Technical Report No. 7

Prepared for

ADVANCED RESEARCH PROJECTS AGENCY
1400 Wilson Boulevard
Arlington, Virginia 22209

Monitored by

AIR FORCE CAMBRIDGE RESEARCH LABORATORIES
AIR FORCE SYSTEMS COMMAND
UNITED STATES AIR FORCE
BEDFORD, MASSACHUSETTS 01730

ARPA Order No. 2055

Program Code No. 3D10

Effective Date of Contract 1 June 1972

Contractor: University of Southern California

Contract No. F19628-72-C-0275

Principal Investigator and Phone No.
Prof. F. A. Kroger/213 746-6224
Prof. John H. Marburger/213 746-2227/9

AFCRL Project Scientist and Phone No.
Alfred Kahan/617 861-4014

Contract Expiration Date 30 November 1973

CONTENTS

1. INTRODUCTION

The format of this report follows closely that of the first quarterly report in which projects are identified by codes keyed to the contract work statement.

The various categories are briefly:

a) Crystal growth
b) Polycrystalline window fabrication
c) Mechanical properties of window materials
d) Window material defect characterization
e) Theory of residual IR optical absorption
f) Absorption measurement techniques
g) Theoretical evaluation of optical performances of windows

a.1 Use of Zirconia as Gages and Pumps for GaAs Epitaxial Growth

S. T. Hoelke, P. S. Vijaykumar and J. M. Whelan

In previous reports, the use of stablilized zirconia has been described as a means for monitoring the purity of H_2 atmospheres under which epitaxial films of GaAs were grown from Ga solutions by dipping and for removing oxygen from the solutions by electrolytic pumping. Interest in oxygen as a possible impurity responsible for its semi-insulating properties has been reviewed also.

It was shown that none of the GaAs samples with unusually low absorption coefficients at 10μm contained oxygen at concentrations in excess of their combined silicon and aluminum concentrations. Furthermore, it was shown that silicon at concentrations of 0.1 ppm can react with oxygen in Ga melts and hence be eliminated as an impurity if the oxygen fugacities are controlled for growths at 600 - 700°C.

A solution-epitaxy apparatus using sections of zirconia cylinders as pumps for removing oxygen from Ga melts used for epitaxial growth was described in the past report. Evaluating it during this period was severely complicated by failures of zirconia pumps/gages used to purify and monitor the H_2 atmospheres over which the growths would be done. Eight pump gages of various designs failed because of cracking and leaking of the tubes. In spite of this, the potential utility of these devices was reaffirmed. Cell emf's were stable to within 1mv at 600° which permitted the detection of changes in H_2O concentrations of 5% at levels of 1-10ppm. Guidelines which have evolved during this period for using the gages are: (1) avoid thermal cycling and thermal shocks; (2) use thermal gradients as small as possible; (3) use reference gas mixtures in the reference electrode such that the oxygen fugacities on the inside and outside surfaces of the zirconia are as small as possible, $\sim$ 6 orders of magnitude or less; (4) arrange the gas handling system such that the gage/pumps can be removed from service without temperature changes for leak testing. The recent reference gas mixtures of H_2O/H_2 made by bubbling H_2 through H_2O at 0°C have been unsaturated except for H_2 flows of $\sim$ 1cc atm/min. A new bubbler in which near saturation is achieved at room temperature followed by condensation at 0°C will be used shortly. Although the gages have presented problems they have helped to diagnose difficulties with a new system for the growth of epitaxial semi-insulating GaAs. These included the detection of leaks in two H_2 electrolytic/pd diffuser generators and the severe outgassing of the Poco DPF-1 carbon used in the slider apparatus noted above.

Designs have been completed for the elimination of the carbon parts in

in the apparatus for the growth of semi-insulating GaAs. Replacement materials have been received recently. The gas handling system and furnace have been constructed. The furnace differs from the usual solution epitaxy apparatus in that vertical temperature gradients can be slowly introduced and then maintained so as to provide stability for the growth of thick films.

a.2 Optimization of Alkali Halide Window Materials

P. J. Shlichta, R. E. Chaney

a.2a Summary: Anion-doped KBr crystals have been prepared by pulling crystals from melts of KBr doped with $KBrO_3$ and /or water and by annealing crystals in O_2 and $CO_2 + H_2O$ atmospheres. All such specimens have characteristic ultraviolet absorptions but thus far only the bromate-doped crystal has shown an order-of-magnitude enhancement of 10.6μ absorption which, according to low-temperature infrared spectrophotometry, is caused by the tail of a broad absorption band at 9.8μ. The laser calorimeter is being rebuilt and an apparatus for controlled-contour chemical polishing specimens is under construction. Problems with the crystal pulling apparatus have been overcome and faceted as-grown crystals of KBr are now available for testing. Attempts to purify molten KBr by reaction with CBr_4 vapor have been unsuccessful due to excessive carbonization. Preparations are now underway to attempt the removal of reducible impurities (and hence the reduction of the 10.6μ absorption) by treatment of crystals with potassium vapor.

a.2b Impurity-Induced 10.6μ Absorption in KBr: During the present report period, we have concentrated exclusively on attempting to resolve the thousandfold discrepancy between the theoretically predicted and experimentally measured 10.6μ absorptivity of KBr. This discrepancy is usually attributed to the presence of a polyatomic anionic impurity such as bromate (ref. 1) or the combined action of carbonate and hydroxide (ref. 2). Presumably, such impurities should be substantially removed by treatment of the molten KBr with Br_2 and HBr, such as has been the practice at USC. However, one cannot exclude the possibility that a residual parts-per-billion concentration of such impurities might survive treatment with HBr and might accound for observed 10.6μ absorptivity of $10^{-3}cm^{-1}$. Accordingly, we have initiated the following program:

1. Anion-doped KBr crystals are prepared by:
   - A. Growing crystals from solution.
   - B. Pulling crystals from melts of salt-doped during prior crystalization from solution.
   - C. Pulling crystals from melts treated with impurity-producing atmospheres such as water vapor or CO_2.
   - D. Annealing crystals in impurity-producing atmospheres.
2. Specimens are prepared by:
   - A. As-grown faces.

B. Cleaving

C. Abrasive string-sowing

D. Annealing in appropriate atmosphere

E. Controlled-contour chemical polishing (see below)

F. Ordinary chemical polishing

3. Ultraviolet absorption spectra are used to characterize impurites.
4. Laser calorimetry is used to determine which impurities, if any, enhance the 10.6μ absorption.
5. Confirming and characterizing this absorption by infrared spectrophotometry at liquid helium temperatures.

Thus far, KBr crystals have been grown from pure melts pertreated with HBr or HBr + Br_2; from pure vacuum-dried untreated melts; and from untreated melts of bromate-doped material. Samples cleaved from commercial crystals have been annealed at 600°C in atmospheres of O_2 and $CO_2 + H_2O$.

Ultraviolet absorption spectra were determined for unannealed cleaved samples of all of the above. By far the cleanest spectrum was that of the crystals grown from purified pretreated melts; these had a single sharp absorption edge at about 2100 Å. One of these crystals (3-3C) was used as a reference standard for running differential spectra of the other specimens. The resultant spectra are shown in Fi,ure a.2.7 and summarized in Table a.2.1. Nearly all these specimens - the as-received otpovac material (Optovac 9), the $CO_2 + H_2O$ treated optovac material (optovac 10) and the crystal pulled from untreated salt (3-7) all show an augmented absorption edge at 2100-2200 Å, 2500-2600 Å and around 3500 Å. The shoulders at 2200 and 2500 Å appear to be most intensely present in the optovac sample heated in dry oxygen (optovac 11). (It should be noted that the difference in spectra between the a and b directions in Optovac 10 and 11 are consistent with the assumption of a finite-diffusion zone in the gas-annealed samples). In contrast to these specimens, the bromate-doped crystal (3-6) shows no low-wavelength edge but rather a well-defined peak at 2200 Å with a shoulder at 2500 Å. It is as yet uncertain whether these peaks correspond to BrO_3^- or whether they correspond to the shoulders observed in the O_2-treated and as-received Optovac samples. Although the position of the 2100-2200 edge corresponds to that of the hydroxide peak as determined by Rolfe (ref. 3), it is unlikely that this peak would be reduced by treatment with moist CO_2. The proper interpretation of the UV spectra in these specimens will require considerable additional work.

The 10.6μ absorption of these specimens, as determined by laser calorimetry

and listed in Table a.2.1, has thus far disclosed only one significant impurity effect; i.e. that the bromate-doped specimens have an apparent β , an order of magnitude greater than any other specimen. The infrared transmission spectrum of this specimen at 77°K shows three broad absorption bands centered at approximately 9.2μ, 9.8μ, and 12.7μ (figure a.2.2). At room temperature, these bands smear out so that the long wavelength tail of the 9.8μ band obviously contributes to the absorptivity at 10.6μ.

The concentration of bromate ion (or its decomposition product), in specimens 3-6 is estimated to be less than 10^{-4}. On the other hand, the concentration of bromate in reagent grade KBr is about 10^{-5} and it is questionable whether our present purification procedures reduce this concentration by more than a factor of ten. It is therefore reasonable to conjecture that the bromate present as an impurity may account for some or even all of the anomalously high 10.6μ absorption observed thus far in KBr. To test this hypothesis, bromate-doped KBr will be prepared both by doping melts prior to crystal pulling and by pressing polycrystalline disks of KBr crystallized from bromate-doped solutions. Since it is still possible that other anionic impurities also contribute to the 10.6μ absorption, the growth and evaluation of KBr crystals doped with other anions will continue.

a.2c Crystal pulling: It was originally intended that infrared absorptivity measurements would be made on as-grown faceted crystals so that the effects of surface and bulk damage from cleaving and polishing could be eliminated. Our failure thus far to produce such crystals has been one of the major disappointments of this phase of the program. Until recently, despite various modifications of our pulling apparatus, we were only able to pull rounded crystals at rates of a few millimeters per hour. It was suspected that this difficulty was in some way a consequence of our having designed the apparatus so as to have no contaminative materials (e.g. metals) in the crystallization chamber. It was presumed for example that the fused silica pull rod did not provide adequate heat conduction away from the growing crystal. Replacement of the solid rod by a hollow air-cooled silica tube resulted in negligible improvement in pull rate. Replacement of this by a water-cooled inconel pull rod caused an appreciable but still inadequate improvement. Moreover, the inconel rod, even when rhodium plated, was attacked by bromine vapor.

These unsuccessful modifications convinced us that the trouble lay in the transparent radient-heat furnace (ref. 4) which evidently had a far flatter temperature profile than conventional resistance furnaces of the same size. Accordingly, two modifications were made: (1) the helical heating coil was replaced by a "hairpin" coil which permitted unobstructed viewing of the

crucible from any vertical angle, and (2) the crucible was placed near the top of the coil which in turn was placed near the top of the reflection chamber. These modifications have apparently solved the problem, inasmuch as faceted crystals can now be grown at rates in excess of 2cm/hr.

a.2d Treatment of Molten KBr with Reactive Vapors: As reported previously, attempts to purify molten KBr with ethyl bromide vapor were unsuccessful due to carbonization of the ethyl bromide and consequent contamination of the melt with carbon particles. During the present period, an attempt was made to treat molten KBr with CBr_4 vapor, by placing powdered KBr in the growth chamber just below the crucible. At about 200°, the CBr_4 vaporized. As the temperature approached 500°C, bromine vapor, apparently due to CBr_4 decomposition, became visible and at 600°C, the walls of the chamber became coated with carbon. Moreover, the metal pull rod was severely corroded. We do not plan any further experiments with organic bromides, especially since, in our opinion, the removal of impurities such as bromate ion might better be achieved by treatment with a strong reducing agent such as potassium vapor. Apparatus for such treatment is now being assembled.

a.2e Annealing and Polishing of Calorimetric Specimens: During our earlier work with KCl, we resorted to the convenience of using as-cleaved samples. Although the bi-refringence caused by cleavage is undoubtedly a contributor to light-scattering and hence to calorimetric error, the calorimetry of KCl cleaved samples appeared to give reasonable linear absorption vs. thickness extrapolations for determining surface and bulk absorptivities.

KBr, however, is much softer than KCl, and therefore much more susceptible to cleavage damage. Examination of our cleaved specimens in a schlieren apparatus showed extensive light scattering and attempts to determine bulk absorptivity by linear extrapolation of absorption vs. sample thickness have too much scatter to be believable. Accordingly, our calorimetric specimens are now being preprocessed by annealing for 2 to 20 hours in an inert (or suitably reactive) atmosphere and by controlled-contour chemical polishing of the optical surfaces. With regard to the latter technique, the porous-plate apparatus, described previously (ref. 5) is being replaced by one in which the specimen is slowly translated into a centrifugally spreading film of solvent on a rotating glass disk. This apparatus is now being assembled and will be tested and evaluated during the next report period.

References

1. T. F. Deutsch, Third Conference on High-Power Infrared Laser Window Materials, November 12-14, 1973, Volume 1, (14 February 1974) pp. 13-30; verbal remark not included in published proceedings.
2. H. G. Lipson, J. J. Larkin , and B. Bendow, ibid, pp. 237-265.
3. J. Rolfe, Canad. J. Physics, 41 (1963), pp. 1525-7.
4. T. B. Reed, Solid State Research Report (Lincoln Laboratory, MIT) (1973),p.1.
5. P. J. Shlichta, and R. E. Chaney, IR Window Studies; Quarterly Technical Report No. 5, (in September 1973), p. 13, 19.

KBr

CRYSTAL OR SOURCE OF MATERIAL	HISTORY	CLEAVAGE	THICKNESS (cm)	UV ABSORPTION SPECTRA (Compared to 3-3C) (See Figure a.2.1)	AVERAGE β AT 10.6μ FROM LASER CALORIMETRY ($\times 10^{+3} cm^{-1}$)
3-2	Pulled from purified melt pretreated with HBr and Br_2-silica crucible.	A	.274		
		B	.389		3.45 to 4.14
3-3	Pulled from purified melt pretreated with HBr - carbon crucible.	A	.332	reference sample: sharp 2000 Å edge with no structure at longer wavelengths.	6.20 to 6.63
		B	.563		1.10 to 2.97
		C	.613		4.36
3-6	Pulled from melt of KBr crystallized from bromate-doped solution (1 mol %); vacuum dried, no gas pretreatment.	A	.665	No edge below 2100Å. Broad peak at 220A, shoulder at 2500Å.	69.0
		B a direction	.561		29.3
		b direction	.686		52.0
3-7	Pulled from purified melt; vacuum dried, no gas pretreatment.	A	1.07	Intense broad edge at 2000-2200Å, shoulder at 2500-2600.	
Optovac 8 (Random cleavage)	As-received: cleaved to size	A a direction	1.55		4.13
		b direction	1.14		3.55
		c direction	0.70		8.23
Optovac 9 (Cleaved rod)	As-received: cube cleaved from center.	B a (through annealed faces)	1.03	Intense 2100Å edge with 2200Å and 2600Å shoulders, small 3000A shoulder.	
		b (through cleaned faces)			
Optovac 10 (Cleaved rod)	Annealed 200 hours at 600°C in H_2O-saturated CO_2 atmosphere: cube cleaved from center.	B a (through annealed faces)	1.07	Broad edge at 2100-2200Å, shoulder at 2500-2600A	
		b (through fresh-cleaved faces)	1.12	Small 2100A edge, broad 2600 peak with 2400 shoulder	
Optovac 11 (Cleaved rod)	Annealed 150 hours at 600°C in O_2 atmosphere: cuba cleaved from center.	B a (through annealed faces)	1.04	2000Å edge with shoulders at 2100A 2200A, 2600Å, and 3500A	
		b (through fresh-cleaved faces)	1.29	2100Å edge with shoulders at 2300A 2600A and 3500Å	

TABLE a.2.1

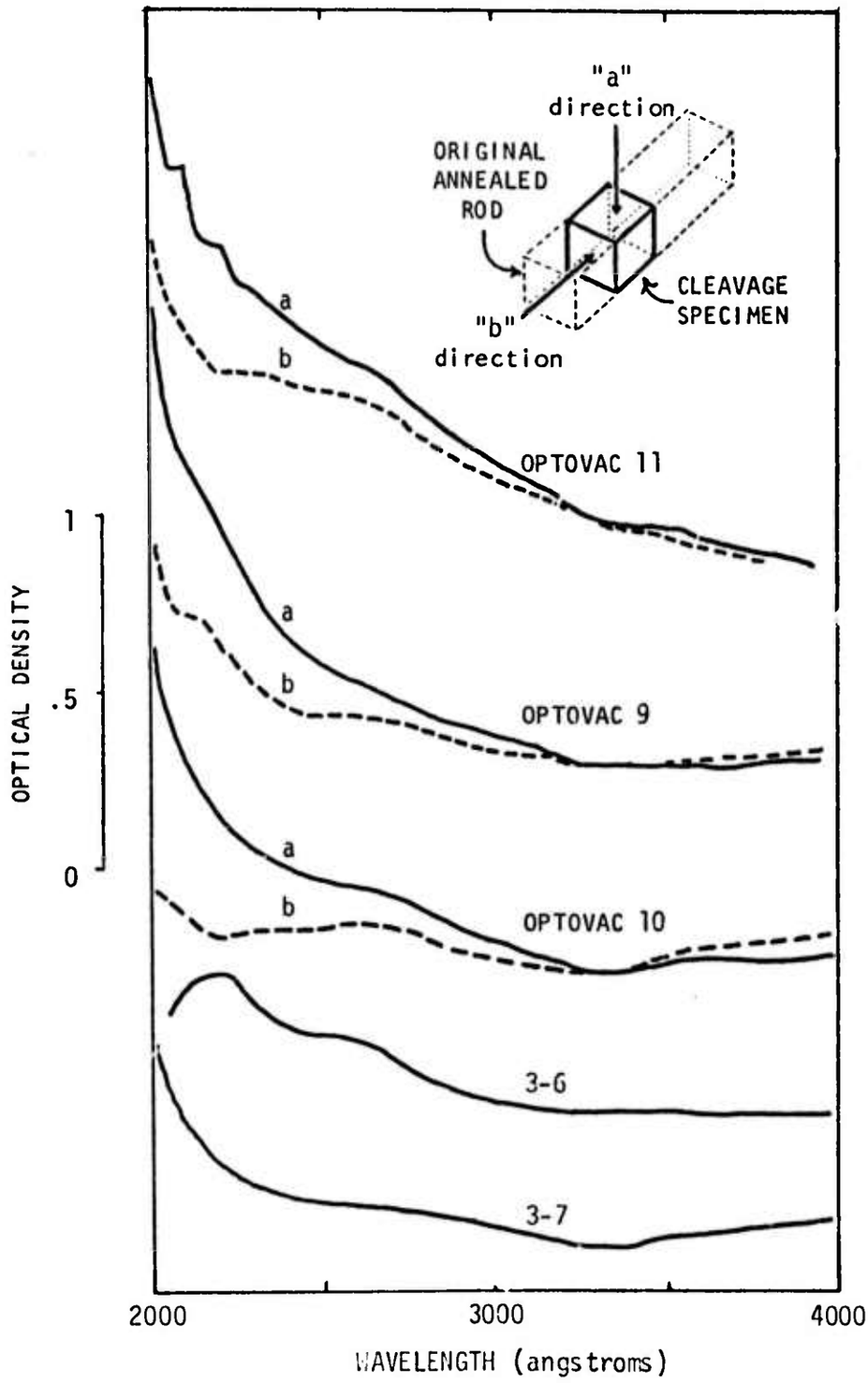

FIGURE a.2.1 Ultraviolet Absorption of KBr Specimens

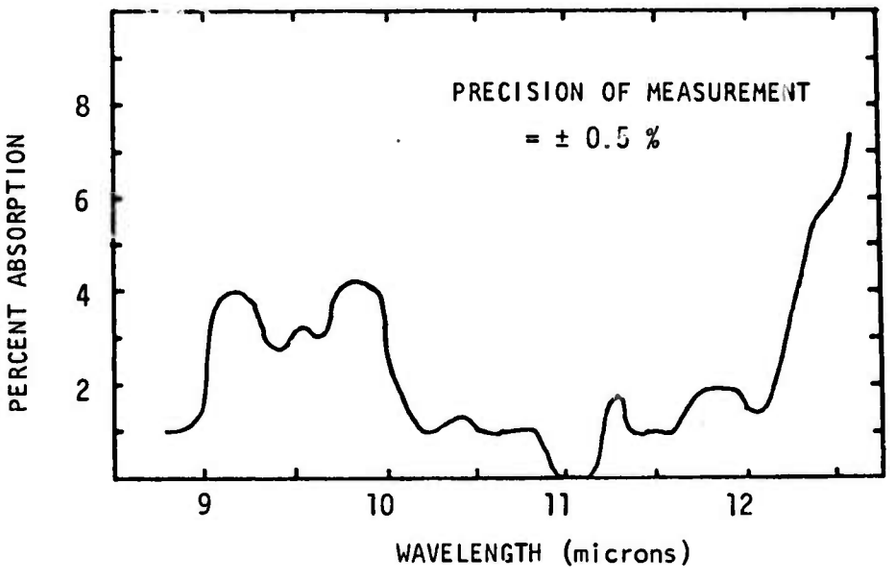

FIGURE a.2.2 Infrared Absorption of KBr Crystal Grown from Bromate-doped Melt. (Measured at 78°K).

b.1 Fabrication of Polycrystalline IR Window Material

S. M. Copley, J. M. Whelan, and V. Rana

This part of the program is concerned with producing polycrystalline CdTe by compacting a powder mass in the presence of a volatile sintering aid.

Compaction of the powder can be achieved either by hot pressing the powder or by cold pressing it and then sintering. In the present work excess Cd or Te is being used as a sintering aid. The temperatures used during the hot pressing or the cold pressing/sintering operation are such that the excess Cd or Te is present as a liquid phase. Advantages of liquid phase sintering over 'normal' sintering are well known.

This excess Cd or Te will be subsequently driven off during a post-curing operation.

I. Starting Material: CdTe used in the present work is either purchased as single crystal bulk from II-VI, Inc., or is synthesized from high purity elements in the laboratory here.

A. Synthesis of CdTe: Both elemental Cd and Te used for this purpose were of 99.9999% purity purchased from Comincs, Inc.

The quartz tube used for synthesis was cleaned with acqua regia and HF and then washed in deionized water.

Cd and Te have a tendency to stick to quartz because of the presence of CdO or TeO_2 layer on the surface. This weakens the quartz when used above 1000°C. To prevent such sticking, the quartz tube was coated with pyrolytic graphite.

Near-stoichiometric amounts of Cd and Te were placed in the quartz tube which was then sealed under a vacuum of 6×10^{-6}mm of Hg. The tube was then placed in a vertical furnace for synthesis of CdTe.

Starting from 500°C the temperature was raised in the increments of 100°C to 1000°C, the material being held at each temperature for at least 24 hours.

At low temperatures a layer of CdTe forms around Cd particles which slows down the reaction between Cd and Te. So the reactants should be kept for a long time at low temperatures for reaction to go to completion. If the reactants are heated to 1000°C rapidly, Cd remains unreacted because of the surrounding skin of CdTe. At 1000°C, the CdTe skin develops cracks so that Cd and Te react spontaneously, producing a large amount of heat since the reaction is exothermic. This expands the gases present in the vessel suddenly, resulting sometimes in an explosion.

After the synthesis was complete, the material was homogenized at 1100°C. The product was checked by the x-ray powder method and found to be CdTe; no extra peaks were observed.

II. Powder Production: CdTe was obtained in powder form by ball milling bulk CdTe in a tungsten carbide ball mill. To achieve efficient ball milling, bulk CdTe was first crushed to smaller size. It was then loaded in the WC ball mill jar in an appropriate amount such that its volume was approximately 25% of that of the volume of the balls. During milling the balls should be well coated with the powder so that there is no direct contact between the WC balls and the lining of the jar. This minimizes contamination. Any impurity picked up by the surface of the powder may be preferentially dissolved in the liquid phase during the sintering operation due to the solvent extraction action of the liquid.

A high purity approach would be to use CdTe powder, obtained by chemically precipitating the compound from its solution. One such product, a CdTe powder of 99.999% purity is sold by ROC/RIC, Inc. We have used this powder also in the current research, but found that at present there is poor quality control of the product. However, the very fact that a reasonable purity is claimed, indicates that the unavailability of high purity powder is not one of the limitations of the present approach of obtaining polycrystalline CdTe.

III. Particle Size Analysis: The particle size distribution of the ball milled powder was determined by sieve analysis or by visual observation in a microscope. Figure 1 shows a typical particle size distribution.

IV. Hot Pressing: Hot pressing operations were performed on the hot press described in an earlier report.

About 5 grams of CdTe powder of a known particle size distribution is mixed with an appropriate amount of Cd or Te, to yield a compact 1/2" diameter by 1/4" high. This material is pressed in a single action graphite die, at a high temperature in an atmosphere of Argon.

Some runs were made using 2 vol% Cd with CdTe powder, the pressing being performed at temperatures around 500°C. It was found that the Cd liquid did not wet the CdTe particles at this temperature. On applying pressure most of the cadmium squeezed out of the powder mass, any cadmium remaining was in pockets (see Figure 2). This phenomenon is further discussed below in Section V.

Sample No.	CdTe Particle Size	Vol% Cd	Temperature	Pressure	Density of compact
A	-44μ	2	465°C	3500 psi	5.39grms/cc
B	-149μ ,+44μ	5	500°C	3500 psi	5.49grms /cc

Microstructure of sample A, after hot pressing, is shown in Figure 3. Note the presence of pores at grain boundary junctions.

V. Wetting Experiments: Since both Cd and Te have some solubility for CdTe, it is to be expected that both liquids will wet CdTe particles. The non-wetting of CdTe particles by Cd could be due to the oxide layer present on both CdTe and Cd.

There is no data in literature, at present, regarding the energies of Cd (Liquid)/CdTe (Solid) and Te (Liquid)/CdTe (Solid) interfaces, and how they change with temperature. In other words, wetting in these systems has not been investigated at all.

We have done some preliminary experiments in the lab here to investigate the wetting behavior.

(i) $Cd_l/CdTe_s$ System: Experimental set up is shown in Figure 4. Quartz tube was closed under a vacuum of 6×10^{-6}mm of Hg. Evaporation of Cd drop was avoided by keeping excess Cd at a slightly higher temperature.

(a) In Vacuum:

Temperature of Cd_l/Cd_s System	Time kept at that Temperature	Remarks
400°C	1 hour	No wetting, not even sticking
500°C	1 hour	No wetting, not even sticking
600°C	1 hour	No wetting, not even sticking
700°C	1 hour	No wetting, but there is sticking of Cd drop to CdTe surface (See Figure 5)

(b) In H_2 Atmosphere: The tube was evacuated and filled with 0.1 atmos. of dry H_2 gas.

Figure 6: Shows Cd shot (solid) resting on CdTe substrate at room temperature.

Figure 7: Cd shot sags down as temperature approaches the melting point of Cd.

Figure 8: At about 400°C surface tension of liquid Cd increases*; the Cd liquid dewets CdTe surface to form a nearly spherical ball.

Figure 9: At 600°C Cd drop seems to start wetting CdTe. Note the contact angle.

*Cd is one of the few metals having positive temperature coefficient of surface tension. Surface tension of Cd(liquid) increases with temperature reaching a maximum at 425°C after which it goes down again.

(ii) $Te_l/CdTe_s$: No such dewetting by Te_l or by Cd_l in Figure 8. However, Te liquid starts to wet CdTe solid around 750°C, but still the contact angle is high and the liquid has no tendency to flow over the surface of Cdle.

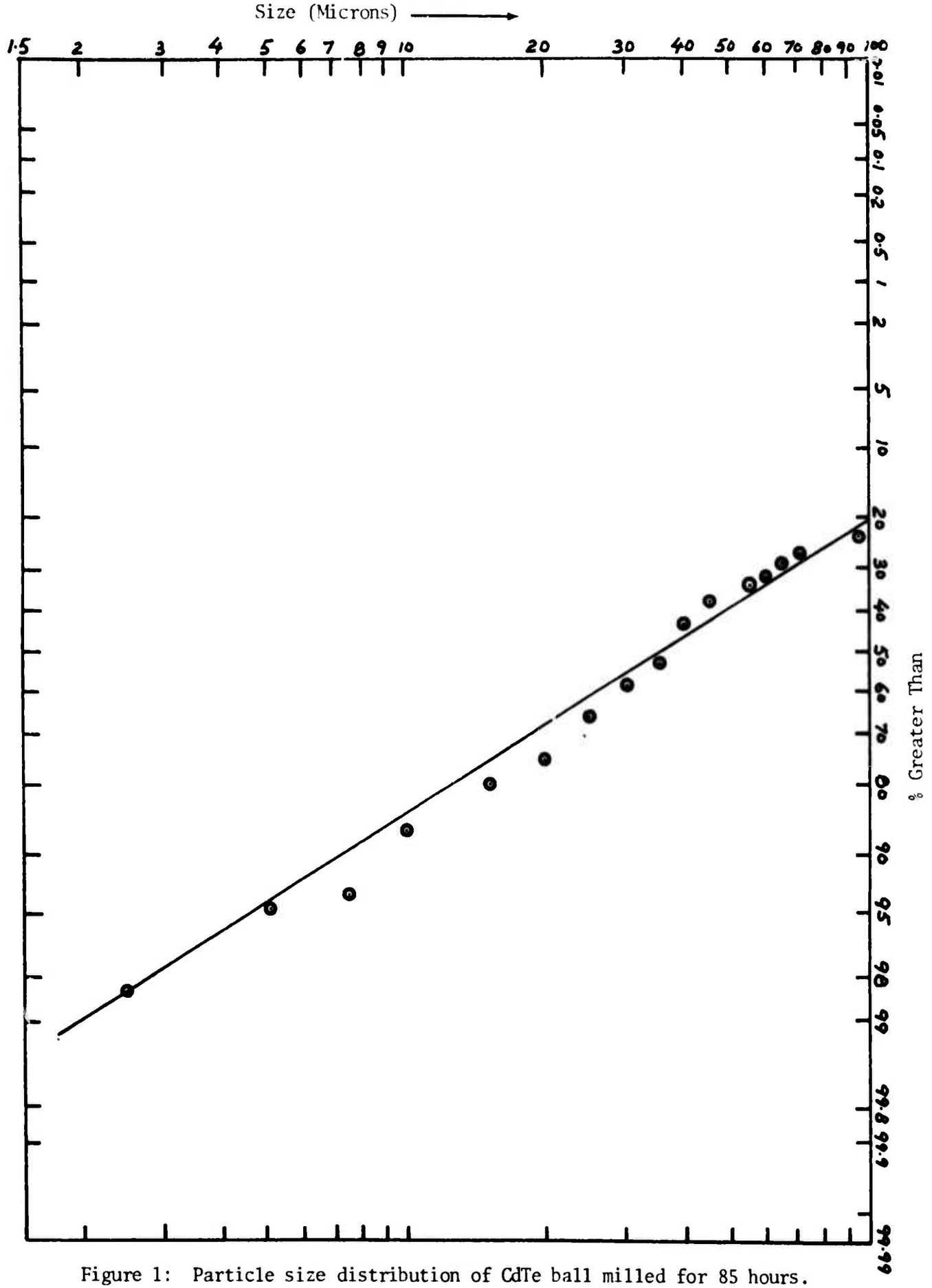

Figure 1: Particle size distribution of CdTe ball milled for 85 hours.

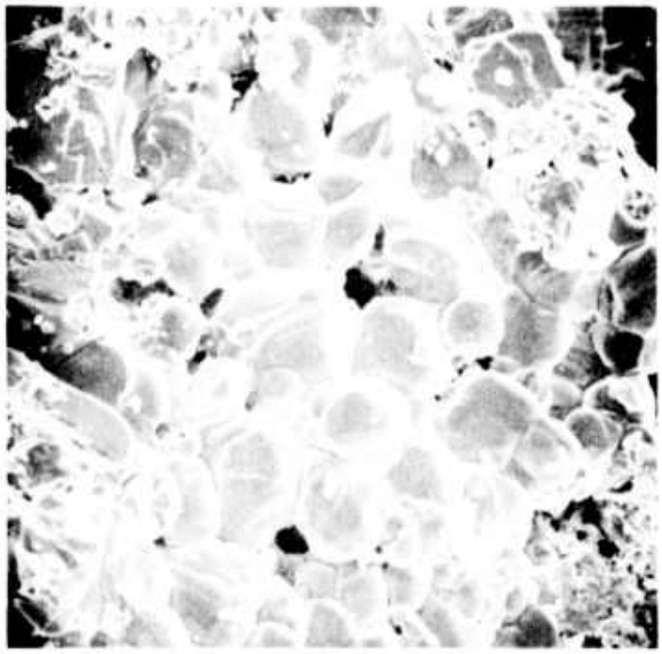

Figure 2: Microstructure of compact B (Mag = 1.5Kx)

Figure 3: Microstructure of compact A (Mag = 4.7Kx)

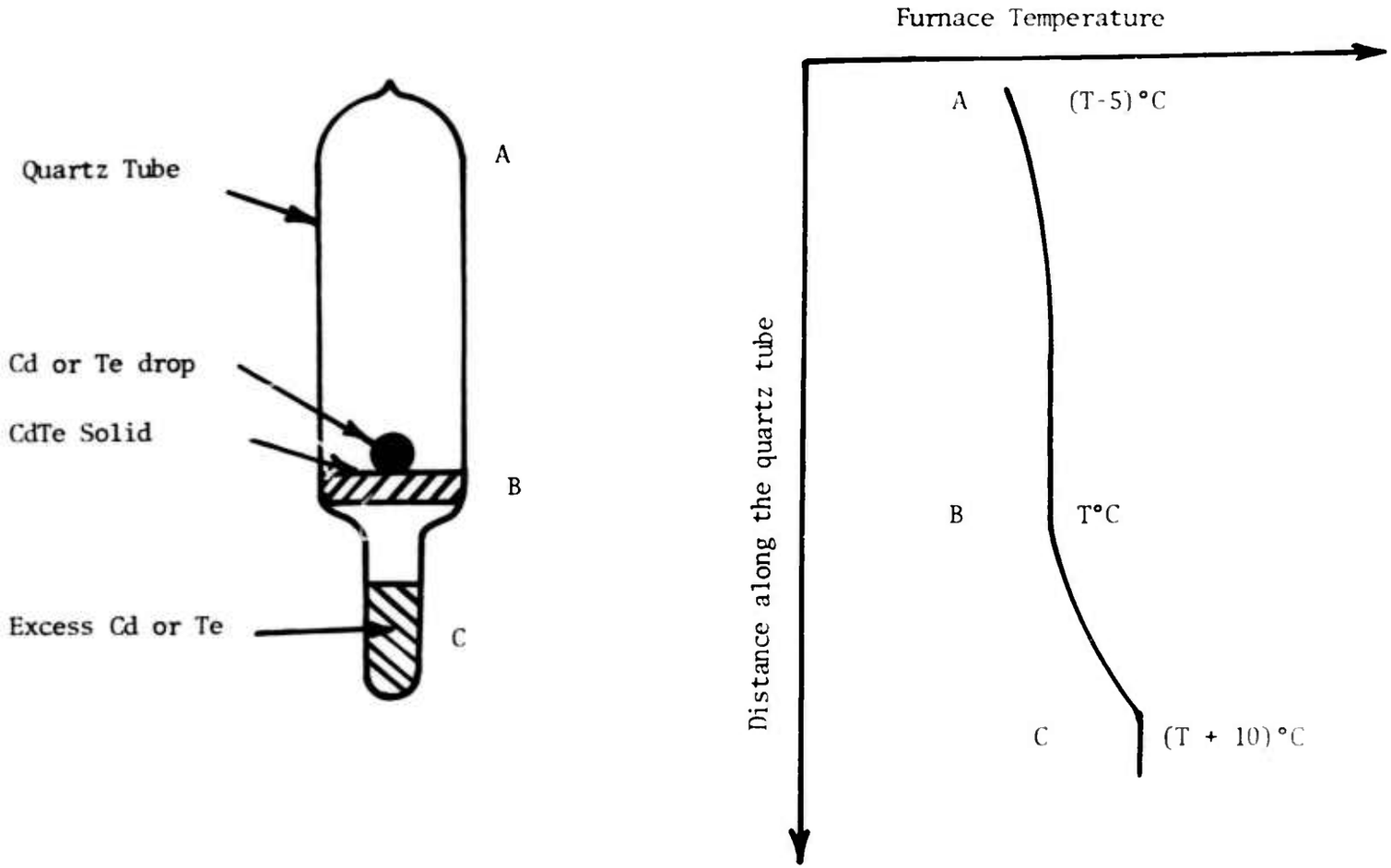

Figure 4: Experimental set up for investigating wetting of CdTe by liquid Cd or Te.

Figure 5: This picture shows the contact angle between a liquid Cd drop and CdTe substrate at 700°C, in vacuum.

Figure 6

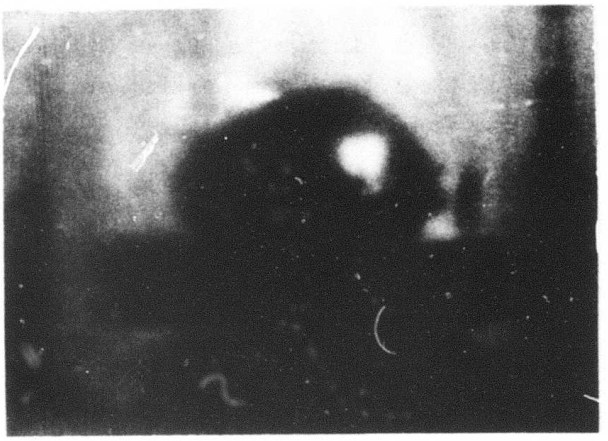

Figure 7

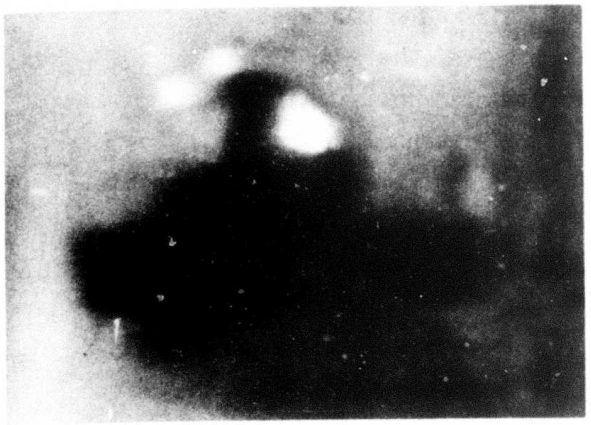

Figure 8

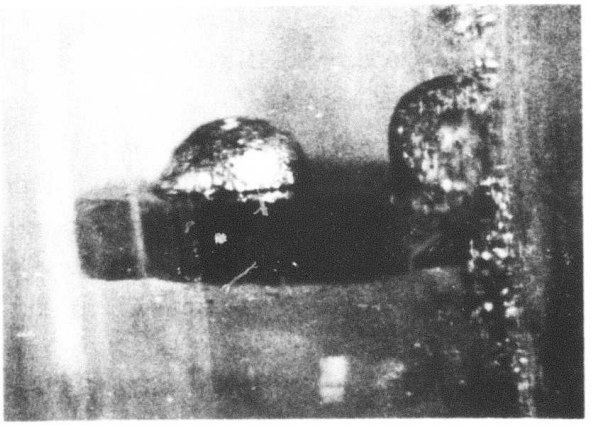

Figure 9

c.1 Mechanical Behavior of II-VI and III-V Compounds

S. M. Copley and V. Swaminathan

In the last quarterly report, we mentioned that the effect of impurities on the yield stress of GaAs is due to dynamic hardening through the formation of tetragonal defects involving vacancy-solute pairs. In this report we will present some recent results that confirm the presence of vacancy-solute pairs.

Stress Strain Experiments: A single crystal of Si-doped GaAs was kindly provided by Professor W. G. Spitzer. Compression specimens having a 111 stress axis and length to width ration of 2:1 were cut with a diamond saw. In order to correlate the mechanical studies with optical experiments by Professor W. G. Spitzer and transmission electron microscopic observation by Professor G. H. Narayanan, the crystal was cut such that all experiments could be performed on adjacent material. The compression specimens were annealed at 1100°C for 15 minutes, so as to achieve the same initial conditions. Stress-strain experiments were carried out at a constant stress rate of 20 psi/sec and at 400°C. The thermal history of the specimens is as follows:

Sample #1: Annealed at 1100°C for 15 minutes and quenched in water.

Sample #2: Annealed at 1100°C for 15 minutes and quenched in water.
Reannealed at 400°C for 68 hours and quenched in water.

Sample #3: Annealed at 1100°C for 15 minutes and quenched in water.
Re-annealed at 700°C for 50 hours and quenched in water.

The variation of annealing was determined from previous studies.[1]

The results of the stress-strain experiments are shown in Figure 1. It should be noted that there is a considerable increase in the yield stress of specimens #2 and #3 as compared to specimen #1. Infrared measurements by Kung and Spitzer[2] indicate the presence of associates of the type Si_{Ga}-V_{Ga} in specimens annealed at 400°C. Their measurements also indicate that the concentration of the associates will be significantly reduced in specimens annealed at 700°C. Therefore, the increase in the yield stress of samples 2 and 3 may be attributed to the dynamic hardening through the formation of Si_{Ga}-V_{Ga} associates, the concentration of such pairs being more in sample 2 than in sample 3. The hardening due to the interaction of dislocations with asymmetrical lattice defects, such as Si_{Ga}-V_{Ga}, is observed in ionic materials[3]. Figure 1 also shows the results of the recovery experiments carried out on samples 2 and 3. The samples were deformed to a few percent of strain, reloaded,

kept at the temperature of deformation for various times as indicated and then reloaded again. It is interesting to note that sample 3 recovers for all time intervals unlike sample 2. The possibility that a component of hardening in this specimen may be to dislocation loops is being investigated.

Future Experiments: Both experimental and theoretical calculations are being carried out to calculate the interaction potential between dislocations and Si_{Ga}-V_{Ga} pairs. Samples are annealed at different temperatures so as to vary the concentration of the pairs. An estimate of the increase in the yield stress as a function of the concentration of associates will be obtained. It has been observed by Narayanan[4] that samples annealed at 700°C contain high density of dislocation loops. The loops themselves being asymmetrical defects can contribute to dynamic hardening. Experiments are in progress to estimate the hardening due to dislocation loops.

References

1. J. K. Kung and W. G. Spitzer, J. Appl. Phys. 44, 912 (1973).
2. J. K. Kung and W. G. Spitzer, to be published in J. Appl. Phys.
3. R. L. Fleischer, J. Appl. Phys. 33 2504, (1962).
4. G. H. Narayanan and A. Kachare, to be published.

d.1 Dielectric Constant Measurements

Clarence R. Crowell, S. Joshi

During this quarter, effort was directed towards characterization of CdTe material and preparation of a dielectric sample. Wafers were cut from a high resistivity CdTe material and were lapped using 3 micron grit size. A wafer was etched using a solution consisting of 10 ml HNO_3; 20 ml H_2O and 4 grams of $K_2Cr_2O_7$. Gold contacts were plated on the sample using $AuCl_3$ solution. This makes ohmic contacts to p-type CdTe[1]. Hall measurements were performed on the sample and resistivity and electron concentration of $2.1 \times 10^8 \Omega cm$ and $1.23 \times 10^8 cm^{-3}$ respectively were obtained. The effective electron mobility was found to be $\sim 240 cm^2/vsec$.

To prepare a dielectric sample, the same wafer on which Hall measurements were performed was again lapped. Both sides of the wafer were polished to scratch free surfaces with optical finish using a solution consisting of equal parts of Mirrolite and Mirrolite-A GaAs polishing compound. Gold films were then vacuum deposited on the sample.

The dielectric capacitance of these diodes was found to be independent of d.c. electric field up to about $\pm 10^4$ volts/cm independent of small signal frequency in the range of 1 MHz to 10 KHz and with Q factors in excess of 100. The taking of data to yield dielectric constant and its temperature dependence is in progress.

Effort was also directed towards preparation of GaAs with optical flatness on both sides at the wafer by carefully polishing both sides by conventional methods. We have succeeded in preparing such samples of 3-4 mils thickness.

In summary a routine technique of polishing CdTe and GaAs and preparing dielectric samples with reproducible electrical characteristics, i.e. capacitance vs voltage and capacitance vs. frequency has been established. Unfortunately, because of lack of control of sample thickness, we have been unable to measure absolute dielectric constant to better than 3-4% error. Initially, we had attempted to make the GaAs sample thicknesses shorter than the bulk Debye screening length. Our samples, however, have shown a bulk dielectric relaxation time corresponding to about 100 Hz at room temperature. Thus, the thickenss criteria initially proposed may be relaxed and we may measure considerably thicker samples than the 3-4 mils samples previously prepared. This should permit sufficient accuracy to produce satisfactory absolute dielectric constant measurements. During the next reporting period the corresponding work for ZnSe will also be initiated.

References

1. Phase Equilibria and Semiconducting Properties of CdTe, D. de Nobel, Philips Res. Reports, Vol. 14, pp. 361-399, 1959.

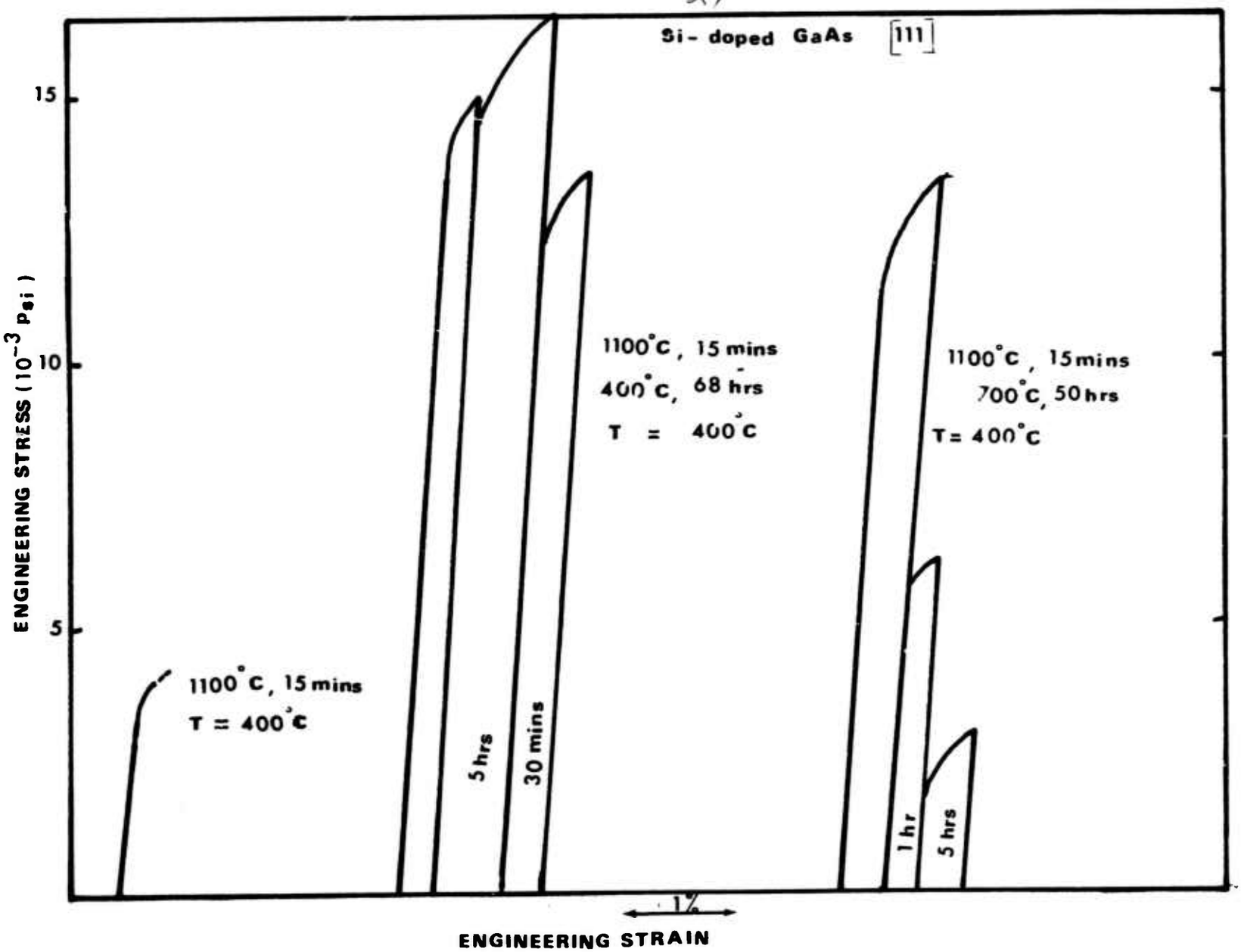
Si- doped GaAs [111]
15
10
5
ENGINEERING STRESS (10^{-3} Psi)
1100°C, 15 mins
T = 400°C
5 hrs
30 mins
1100°C, 15 mins
400°C, 68 hrs
T = 400°C
1100°C, 15 mins
700°C, 50 hrs
T = 400°C
1 hr
5 hrs
1%
ENGINEERING STRAIN

d.2 Study of Defects in II-VI Compounds

F. A. Kroger and F. A. Selim

Crystals of CdTe doped with 5×10^{16} Cl were purchased from the II-VI Company. The crystals were cut into plates of 10 × 10 × 2mm, washed in trichlorethylene ($Cl_2C{:}CHCl$) and etched with a solution of 10 wt % bromine (Br_2) in methyl alchol (CH_3OH).

One crystal was used for the measurement of the Hall effect as $f(P_{Cd})$ at high temperature. Electron concentrations determined from

$$R_W = -(3\pi/8)C_e^{-1}$$

are shown in Figure 1.

Other crystals were enclosed in a quartz tube together with some Cd inserted in a two-temperature furnace and then annealed for two hours at 700°, 800° and 900°C under cadmium pressures between the maximum pressure set by the phase diagram and the minimum pressure region when sublimation occurs. After annealing, the crystals were quickly cooled to room temperature. For each plate, lapping with 3200 mesh abrasive followed by chemical polishing with "mirrolite" was performed. The absorption coefficient was measured by calorimetry using the apparatus set up by Dr. Steier and the free carrier concentration C_e or C_h was determined by measuring the Hall constant. For n-type samples we used indium contacts, for p-type samples gold contacts. The results at 700° are shown in Figure 2. Results at 800° and 900°C were similar, but the absorption was much stronger.

The classical theory for free carrier absorption predicts a λ^2 dependence for the absorption coefficient α[1].

$$\alpha = \frac{Nq^3}{\mu m^{*2}\omega^2\varepsilon_o}$$

N is C_e or C_h, q the electronic charge, μ the mobility of electrons or holes, m* the effective mass, ω the frequency and ε_o, the permittivity of vacuum = 1 in c.g.s. However, the quantum-theoretical calculation predicts a $\lambda^{2.5}$ to $\lambda^{3.0}$ dependence[2]. Whatever the dependence, the absorption coefficient due to holes or electrons at the same wave length (10.6μm) differ only due to the dependence on μ & m*. Therefore, we may write:

$$\alpha = K \frac{N}{\mu m^{*2}}$$

Where N is the free carrier concentration c_e or c_h

$$K = q^3/\omega^2 t_o = \text{constant}$$

Our measurements for Hall effect gave for the mobilities $\mu_e = 640 cm^2 v^{-1} sec^{-1}$ and $\mu_h = 60 cm^2 v^{-1} sec^{-1}$.

Taking $m^*_h/m = 0.35$, $m^*_e/m = 0.14$ (de Nobel[3]) $\therefore \alpha_e = K C_e/12.16$, $\alpha_h = K C_h/7.32$. Therefore, we may write $\alpha = K'(C_e + 1.76C_h) cm^{-1}$[1] with $K' = K/12.16$.

K' can be determined if we know the λ dependence for α. According to Jensen[2], $\alpha \propto \lambda^3$. We are planning to check this relation for carrier concentrations of 10^{13}-10^{16} in which polar optical mode scattering is dominant, and impurity scattering being eliminated as far as possible.

Figure 3 shows the absorption coefficient dependence for both holes and electrons. The absorption due to holes is slightly less than proportional to the carrier concentration, with $\alpha_h \propto C_h^{0.96}$. This corresponds to a proportionality constant varying from 1.76 at $C_h = 2.5 \times 10^{15} cm^{-3}$ to 2.2 at $C_h = 1.35 \times 10^{13} cm^{-3}$ or K' from (1) is $(1.13 \pm 0.12) 10^{-16} cm^2$.

For electrons we were limited to a range from 10^{-1} to less than 0.2 atm. Two experimental points give the relation

$$\alpha = (1.4 \pm 0.1) 10^{-16} c_e cm^{-1} \text{ or } K' = (1.4 \pm 0.1) 10^{-16} cm^2.$$

References

1. Houghton and Smith, Infra-red Physics, Oxford Univ. Press, 1966.
2. B. Jensen, J. Phys. Chem. Solids 34 (1973), 2235.
3. D. de Nobel, Philips Res. Rept. 14 (1959), 361, 430.

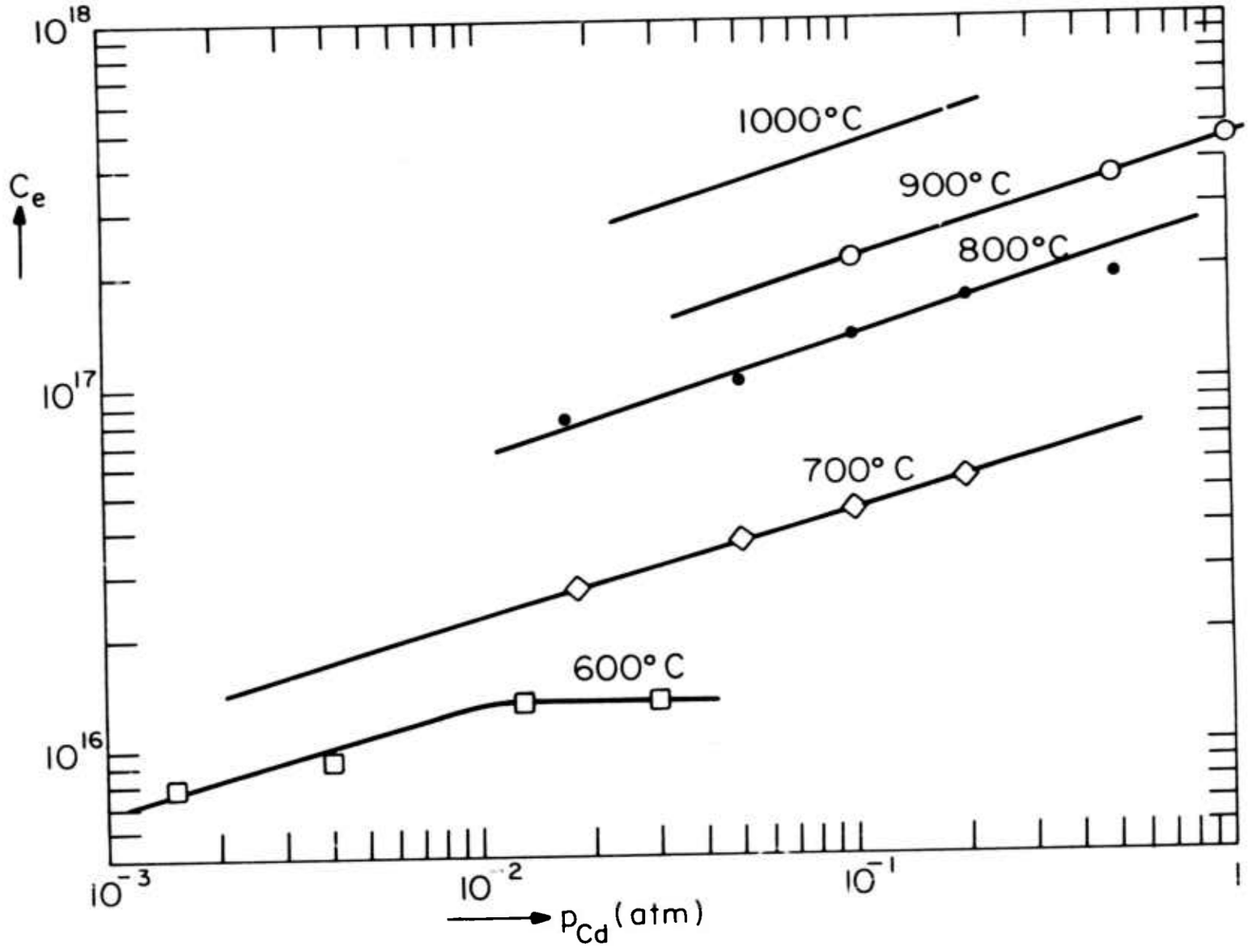

Figure 1: CdTe + 5×10^{16}Ci, Carrier concentrations; determined from the High-Temperature Hall effect

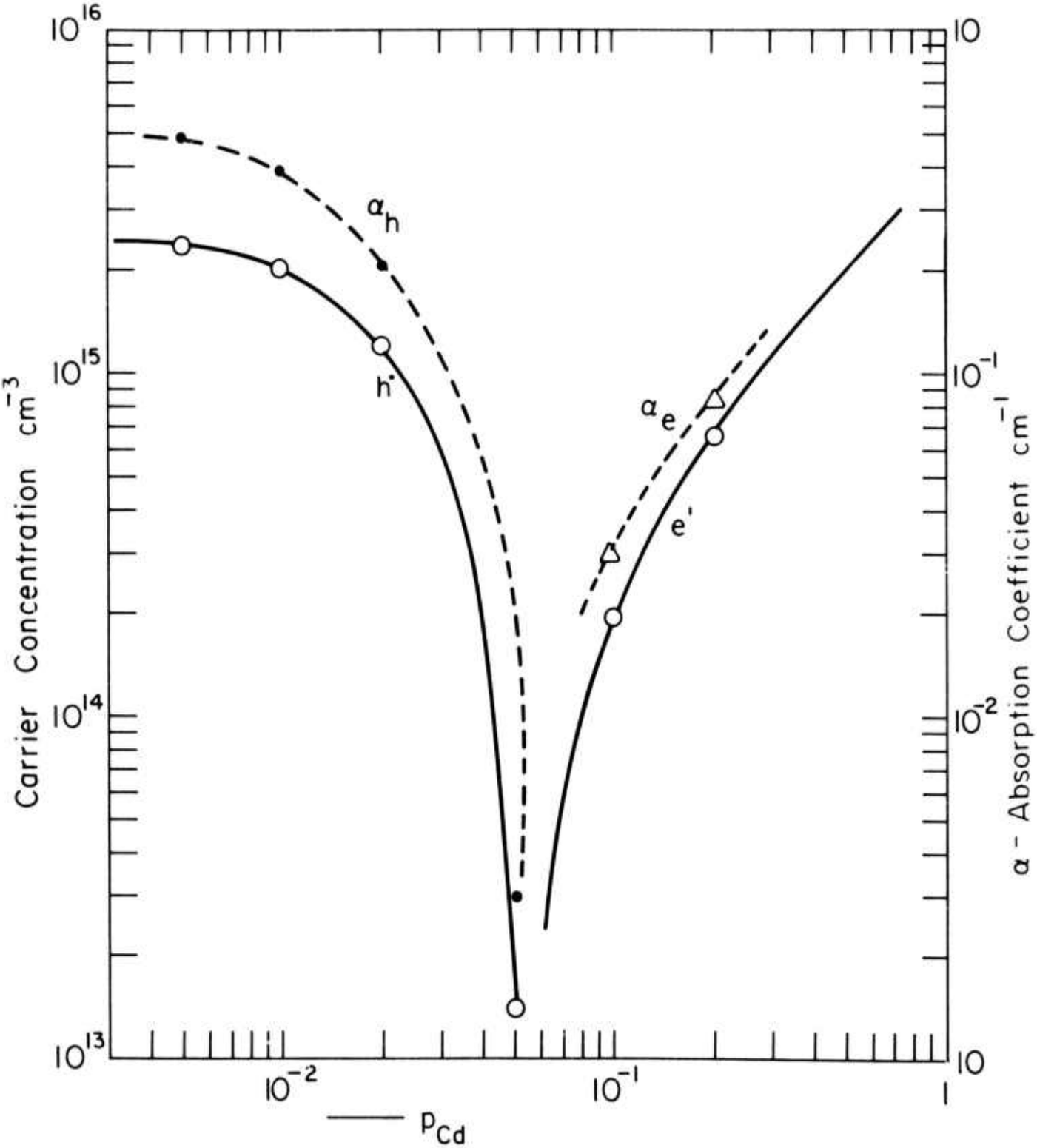

Figure 2: CdTe + 5 × 10^{16} Cl quenched from 700°C

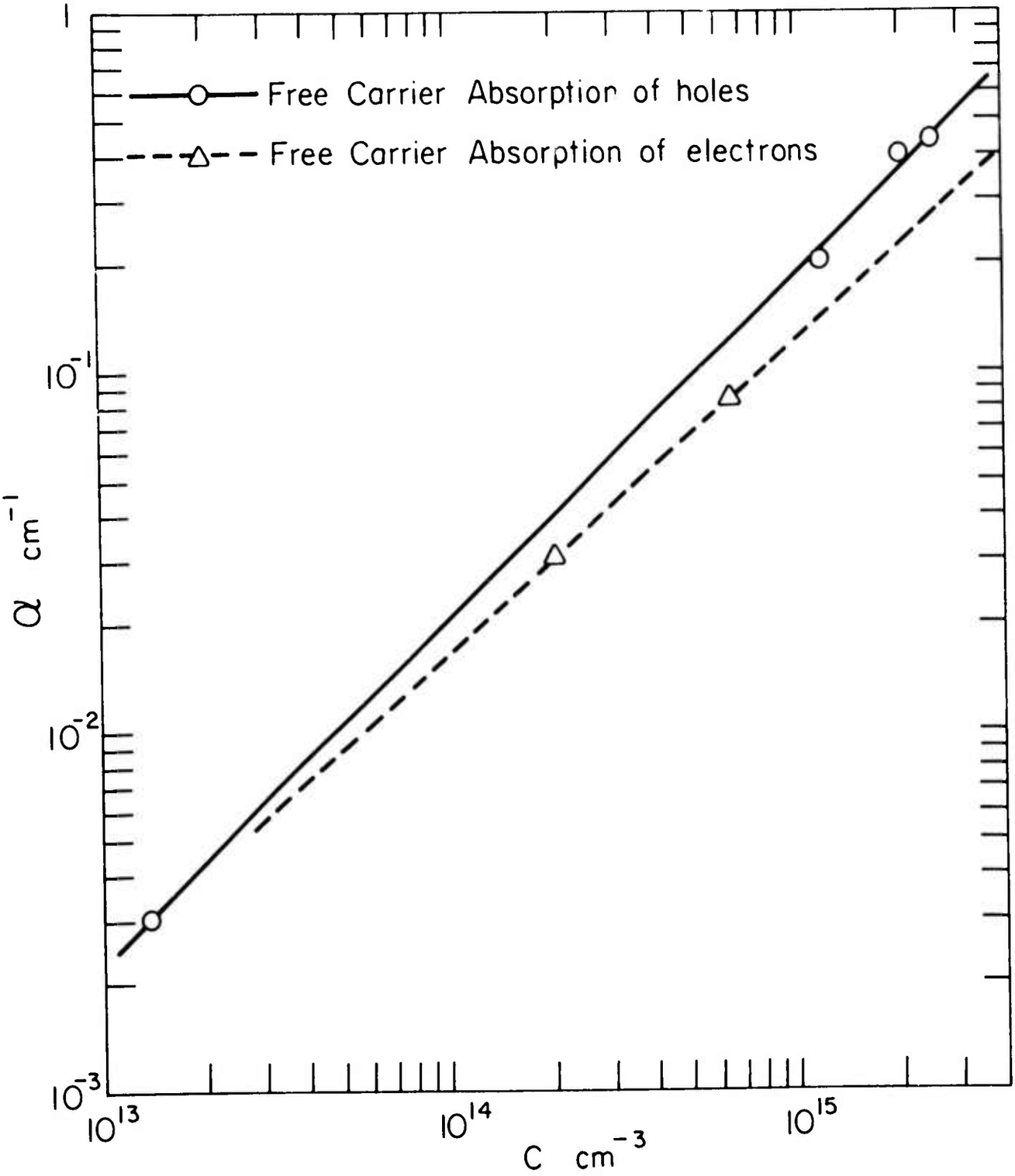

Figure 3: Absorption coefficient of CdTe $+5\times16$Clcm^{-3} at 10.6μm determined by calorimetry as function of carrier concentration (electrons or holes) determined from Hall measurements at room temperature for crystals cooled from 700°C.

e.1 Theoretical Studies of Absorption Mechanisms in IR Window Materials
R. W. Hellwarth and M. Mangir

In this quarter we extended our analysis of the contribution of the nonlinear moment mechanism to multiphonon absorption in LiF. We used the method discovered in the previous period which is based on measurements of the imaginary part ε_2 of the dielectric function over a broad frequency range around ω_{TO} and at high and low temperatures. (To date LiF is the only crystal for which sufficient data exist to apply this method.) Although this method requires a model for the quadratic term in the nonlinear moment, if such moment is large enough to contribute significantly to multiphonon absorption. Previously, we showed that the nonlinear moment is significant in LiF, although an independent-molecule model for it indicated it was of minor importance.

This quarter we developed a very accurate expression for the nonlinear moment contribution (in rocksalt structures) in terms of the measured integral

$$\int_0^\infty \omega d\omega \varepsilon_2(\omega)$$

and certain averages of quadratic products $\vec{x}_\alpha \vec{x}_\beta$ of ionic displacements. We computed these averages for a model lattice having nearest-neighbor springs. Both models gave the same value for the Born effective charge, $e^* = 1.04 \pm 0.01$ electron charges, and also for the contribution of nonlinear moment to the above integral at high temperatures ($2.5 \pm 1.5\%$ at 573°K or 0.23 ± 0.18 of all multiphonon contributions). However, at low temperatures, the improved model gives a smaller nonlinear moment contribution ($0.5 \pm 0.4\%$ rather than $1.0 \pm 0.6\%$ at 77°K). The low value is expected on physical grounds. The difference-band absorption vanishes at low temperatures. The improved model exhibits difference-band absorption (optic minus acoustic), whereas the molecular model has only summation-bands in its multiphonon absorption. The above quoted errors are experimental in origin. Our experience with the two different approximations in estimating the nonlinear moment gives us great confidence in the general accuracy of our method.

Our preliminary results will appear in the Proceedings of the Third Conference on High Power Laser Window Materials (Hyannis, Mass., November 1973) ed. by C. Pitha. Our more complete results are being prepared for publication.

f.1 Wavelength and Temperature Dependent Calorimetry Measurements on GaAs

W. H. Steier, C. P. Christensen, R. Joiner

To conclude our GaAs characterization program, we have obtained an absorption spectrum for a third 54-4A Bell Laboratories sample and in addition have performed annealing studies designed to complement those described previously.

Bell Laboratories sample 54-4A has been described in Q.R. #4. Figure 1 shows the absorption spectrum obtained for this sample and summarizes the results of our calorimetric measurements to date. Sample 54-4A is seen to exhibit a spectrum which closely coincides with that obtained for the other lowest loss samples. We note that we now have five samples representing three laboratories which have nearly identical absorption characteristics.

In previous reports we have discussed irreversible changes in the GaAs absorption spectrum which were brought about by heating the samples to 400°C in air. In the past quarter we have conducted further annealing experiments but in a controlled atmosphere. Bell Labs sample 54-4A, the undoped, low-loss sample discussed above, was sealed in an evacuated quartz ampule, heated to 400°C for 2 hours and allowed to slowly cool. This heating cycle was intended to approximate that used with the samples heated in air. A second sample, Bell Laboratories 55-1A, was sealed in an evacuated quartz ampule with powdered GaAs, heated to 1100°C for 15 minutes and quenched rapidly. This sample had been earlier subjected to four 400°C anneals in air which had resulted in increased bulk absorption. Both samples were chemically polished and measured before annealing and repolished afterward. The absorption spectra obtained before and after annealing are shown in Figure 2.

From the figure it is clear that the 400°C anneal in vacuum produced little or no change in the absorption spectrum of Sample 54-4A. This result implies that the increased absorption obtained by heating in air is due to contamination of the sample by the oven. The oven used in the loss vs. temperature measurements where irreversible heating effects were first observed was constructed of a steel tube, and the sample was held in position by brass supports. We thus suspect either iron or copper contamination. Copper is a very likely candidate since it diffuses very rapidly in GaAs. At 400°C the diffusion length for Cu corresponding to a 1-hour heating is about 2mm, which in most cases is greater than the sample thickness.

The single high temperature annealing experiment is difficult to in-

terpret. If the increased sample absorption due to the earlier low temperature anneals is the result of contamination, the high temperature anneal in the GaAs atmosphere was expected to reduce the absorption or at least result in no further increase in absorption. It may be possible that the continued increase in absorption is the result of another effect which appears only in high temperature anneals.

To completely explain our annealing results will require a number of additional experiments and an investment in time and facilities that does not appear warranted at this time. It is possible that a complete explanation of the effect could alter our general conclusions about GaAs as a window material, but this seems unlikely.

In summary, our experiments on GaAs has yielded the following results:

A. Samples from several laboratories , grown by different techniques and compensated by different methods all show identical absorption spectra with β varying from 5×10^{-3} at 9.3μ to 9×10^{-3} at 10.6μ. The results are shown in Figure 1 and Table 1.

B. The degree of structure seen in the spectra of Figure 1 is consistent with a resonant process such as intrinsic multiphonon absorption or a vibration associated with a bulk or surface impurity.

C. The order of magnitude of the observed β in the 10μ range is consistent with measurements at other wavelengths assuming an exponential frequency dependence which is characteristic of multiphonon loss.

D. The measurements of β as a function of temperature (see earlier reports) can be explained by free carrier generation above 280°C and is consistent with multiphonon absorption at lower temperatures.

This evidence seems to support multiphonon absorption as the primary loss mechanism in low-loss GaAs. While the evidence is not conclusive, it appears the absorption we have observed in the lowest loss samples is intrinsic to GaAs.

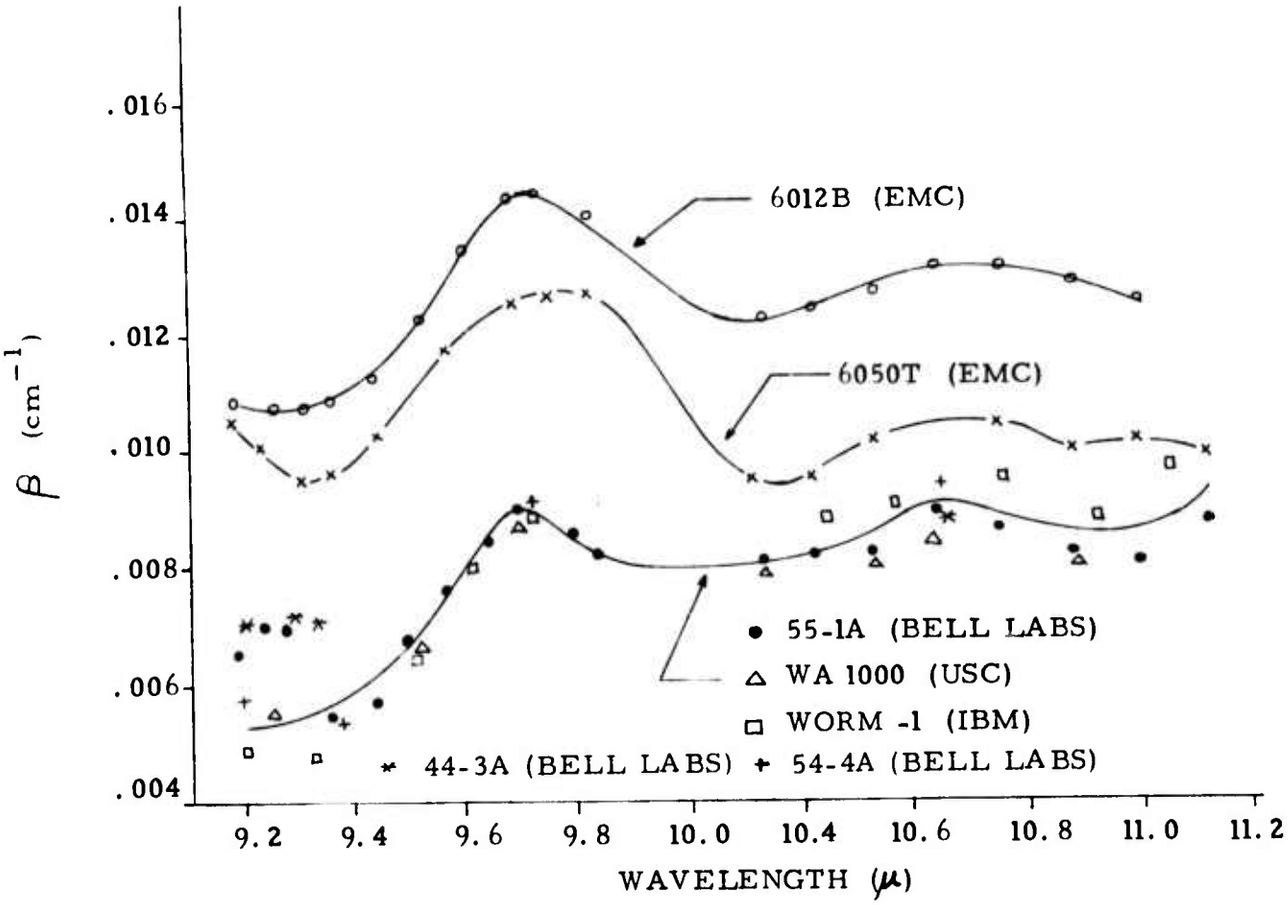

Figure 1. Absorption spectra of GaAs samples described in Table 1.

Sample	Room Temperature Mobility (cm^2/V sec)	Resistivity (ohm-cm)	Growth Technique
Bell Labs 55-1A	6000	1.4×10^8	Float Zone, Un-doped
EMC 6012B	----	2.2×10^7	Czochralski, Cr-doped
EMC 6050T	----	3.2×10^7	Czochralski, Cr-doped
USC WA1000	3000	10^8	Horizontal Bridgeman un-doped
IBM WORM-1	----	high ρ	Horizontal Bridgeman with Oxygen remelt*
Bell Labs 44-3A	5550	4.6×10^8	Float Zone, Carbon-doped
Bell Labs 55-4A	5700	2.5×10^8	Float Zone, Un-doped

TABLE 1. GaAs samples used in calorimetric loss measurements.

*In this sample, oxygen was purposely introduced into the boat, and after growth the sample was remelted.

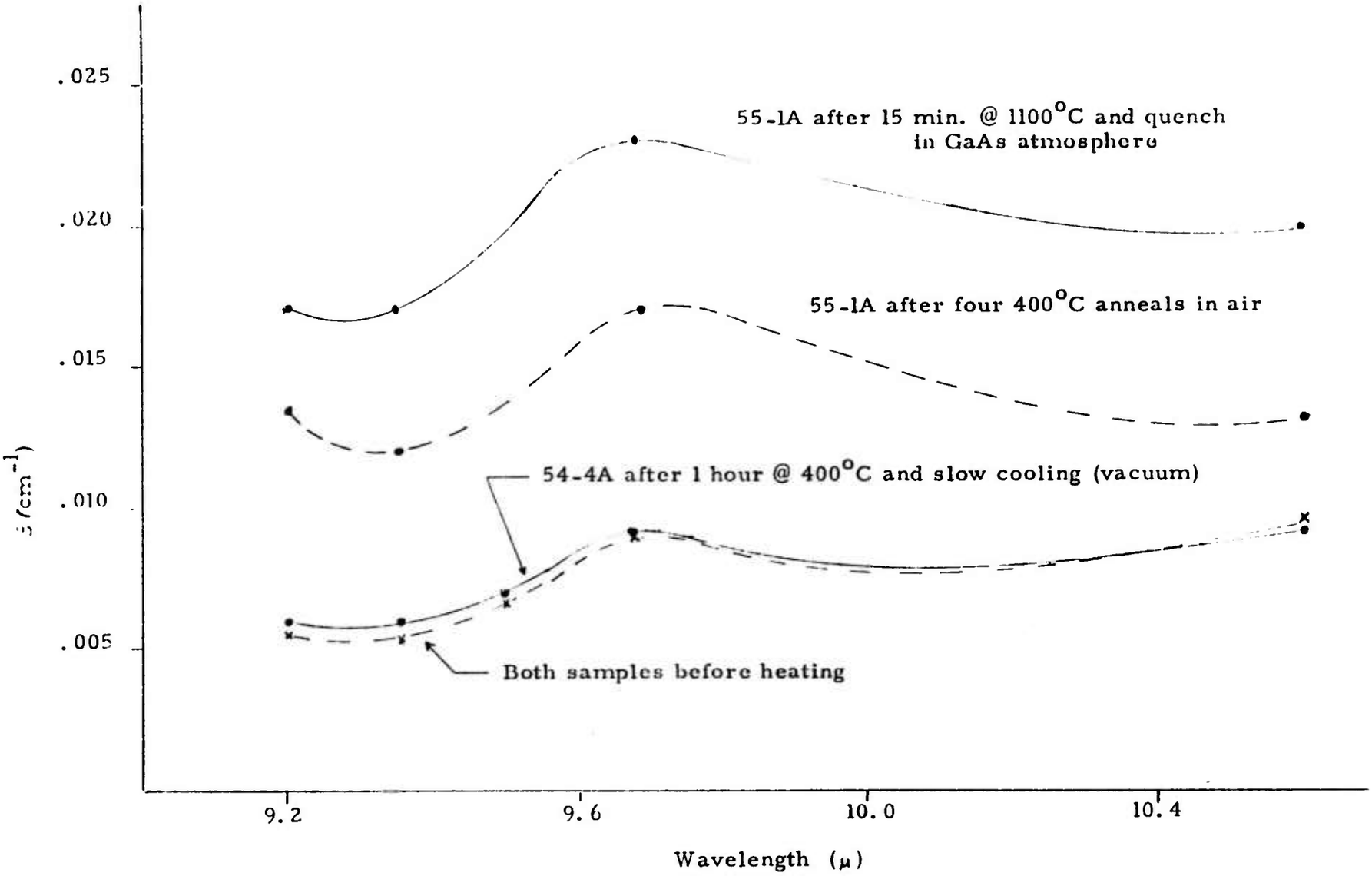

FIGURE 2. Absorption spectra for GaAs samples after annealing

f.2 Acoustic Probe Studies of Surface Properties

T. Colbert, D. Rockwell, J. H. Parks

During this contract period emphasis was placed upon establishing and experimentally verifying a theory for the interaction of an acoustic surface wave with a radiatively heated surface region. It is essential to describe the physical details accurately in order to eventually use the theory to extract reliable surface absorption coefficients. Experimental verification of the theory has been observed to within a 15% systematic discrepancy for 10.6μ laser having widths of pulses $\tau_p \leq$ 10msec and within 5% for greater pulse lenghts.

f.2.1 Theory for a Temperature Induced Phase Shift: A theory has been derived which describes the induced pahse shift of an acoustic surface wave which propagates through a material surface region heated by radiative absorption. An expression for this phase shift has been presented in an earlier report[1] which describes this effect qualitatively. The theory has been modified to include (1) thermoelastic strains accompanying a spatially non-uniform heat distribution, (2) averaging of the phase shift over the acoustic probe width when the temperature distribution varies within this width.

The following expression has been derived for the phase shift $\Delta\phi$ induced by a temperature variation ΔT,

$$\Delta\phi = \frac{2\omega}{V_s} \int_0^L \left\{ \frac{\partial u}{\partial r} - \alpha_v \Delta T \right\} dr$$

This describes the propagation of an acoustic ray between two transducers separated by L on the surface of a cylindrical dish. Part of the phase shift arises from the wave velocity variation with temperature depending on the material coefficient α_v. The contribution to the phase shift from the thermoelastic radial strain has been derived assuming plane stress conditions apply. This strain, $\partial u/\partial r$, represents a constrained thermal expansion of the heated region by the colder surrounding material. In the limit of a spatially uniform temperature distribution $\partial u/\partial r \rightarrow \alpha_L \Delta T$ where α_L is the thermal expansion coefficient.

The effect of thermoelastic strain in the z direction (perpendicular to the propagation direction) and the change of wave velocity induced by thermoelastic stresses are both second order effects proportional to $(\alpha_L \Delta T)^2$ and have been neglected in the derivation.

A gaussian 10.6μ beam of spatial half width a is incident on the substrate

surface area probed by an acoustic wave of beam width w. When a > w, the surface wave phase front will average $\Delta\phi$ given above over the acoustic beam width. To account for this, $\Delta\phi$ is averaged over the portion of the Gaussian profile which is probed by the beam width. It is found that the averaged phase shift $\langle\Delta\phi\rangle$ is proportional to the factor (a/w) which increases the sensitivity of phase shift measurements for the 10.6μ beam geometry.

The temperature change ΔT is generated by the "Heating 3" computer program based on a difference equation solution of the heat equation. The temperature variation used in the expression for $\Delta\phi$ depends on (r,z,t) but ΔT is evaluated at z = 0 for the experiments described below. For the laser pulse widths used in these experiments the diffusion of heat establishes a uniform temperature over the acoustic wave energy profile which extends to a depth less than 10μ below the surface.

The thermoelastic strain contribution and the beam width correction were calculated in a sub-routine to the heat equation program. The phase shift time dependence follows directly from $\Delta T(t)$ and the magnitude of $\Delta\phi$ involves the effect of temperature diffusion.

f.2.2 Experimental Measurements of Temperature Induced Phase Shifts: Temperature induced phase shifts were measured in a highly absorbing material for comparison with the theory outlined above. The axial gradients will be large in this case and heat diffusion in the axial direction will be the primary effect which determines the temperature probed by the acoustic wave for 10.6μ pulse widths greater than 1/2msec. However, a highly absorbing material has the advantage of producing large induced phase shifts for a moderate 10.6μ laser power of several watts. It should be emphasized that such a material offers an opportunity to test the quantitative details of the theory very thoroughly since heat diffusion effects will have to be taken into account accurately and completely to achieve a close correlation with experimental results.

Crystal quartz was chosen as the test material for its high absorption, $\beta = 241 cm^{-1}$ at 10.6μ, and because the optical, thermal and surface wave properties have been extensively studied. In this case the theory - experimental correlation will not depend upon parameter fitting since all the material constants included in the $\Delta\phi$ calculation have been obtained from previous results reported in the literature.

A CO_2 10.6μ laser was constructed which provided single mode power up to 4 watts, a gaussian beam half width of a = 1.4mm, and an average power fluctuation less than 5%. Figure 1 shows the experimental arrangement used to measure the thermally-induced phase shift. The signal from a frequency-locked RF

generator is power divided and half the power is delivered to the interdigital transducer which excites a surface wave on the quartz surface. The other half goes to the left (L) channel of a double balanced mixer and serves as a reference signal. At the receiving interdigital transducer, the surface wave is converted back into an electrical signal, which is amplified and fed into the right (R) channel of the mixer.

The mixer output signal, V_x, is proportional to the cosine of the phase difference between the signals at L and R. A variable external delay line is used to adjust ϕ_R such that the total phase difference $(\phi_L - \phi_R)$ is some odd multiple of $\pi/2$. In this case, additional thermally-induced changes $\Delta\phi_R$ in the phase at R are given by

$$V_x = V_o \cos\left[(2n+1)\frac{\pi}{2} + \Delta\phi_R\right] = V_o \sin \Delta\phi_R$$

The time variation of the surface wave phase is observed by displaying $V_x(t)$ on an oscilloscope. For the phase shifts measured in these experiments, $\Delta\phi_R < .5$ rad and $\sin \Delta\phi_R \approx \Delta\phi_R$ is a good approximation. The amplitude V_o is approximately 340m volts and was checked repeatedly during the experiment.

Figure 2 shows the comparison of experimental results and the computer calculation based on the theory described in section f.2.1. Data for square laser pulses of 100, 50, 10 and 4msec pulse widths are shown. The peak phase shift was measured as a function of the laser power and shows the expected linear dependence of $\langle\Delta\phi\rangle$ on the peak power. The relative variation of the slope indicates the overall effects of axial diffusion. Radical diffusion becomes significant only for the 100msec pulse. Although the 50 and 100msec pulse width data show agreement to within 5%, a systematic discrepancy between theory and data is evident for the shorter pulses. This discrepancy is only about 15%, however it is important to understand how this might arise.

The opening and closing times for the electromechanical shutter are the order of 1msec and although the computer heat function input includes this in the pulse time scale, the computer model is inflexible in one aspect. As the shutter is opening (and closing), the spatial distribution of the 10.6μ beam on the quartz surface is not the full gaussian described by halfwidth a = 1.4mm. In fact, a non-gaussian profile is being established during this time since the most intense central portion of the beam is centered on the shutter and therefore is exposed for the entire duration of opening time. Less intense parts of the beam farther away from center actually are exposed for shorter times. This shutter leads to a non-gaussian heat profile, hotter in the center

and of a smaller halfwidth than a. The important point is that after $\sim$ 50msec radial diffusion has evidently relaxed the heated area to the gaussian beam size. But for the shorter pulses this non-gaussian profile remains and its effect is to reduce the peak value of $\langle\delta\phi\rangle$. The computer program does not offer the possibility of using heating functions other than product functions of space and time, and so this effect cannot be included in the analysis. However, a less accurate, but qualitatively correct analytical calculation does indicate that the net effect is to reduce $\langle\Delta\phi\rangle$ by the percentage observed.

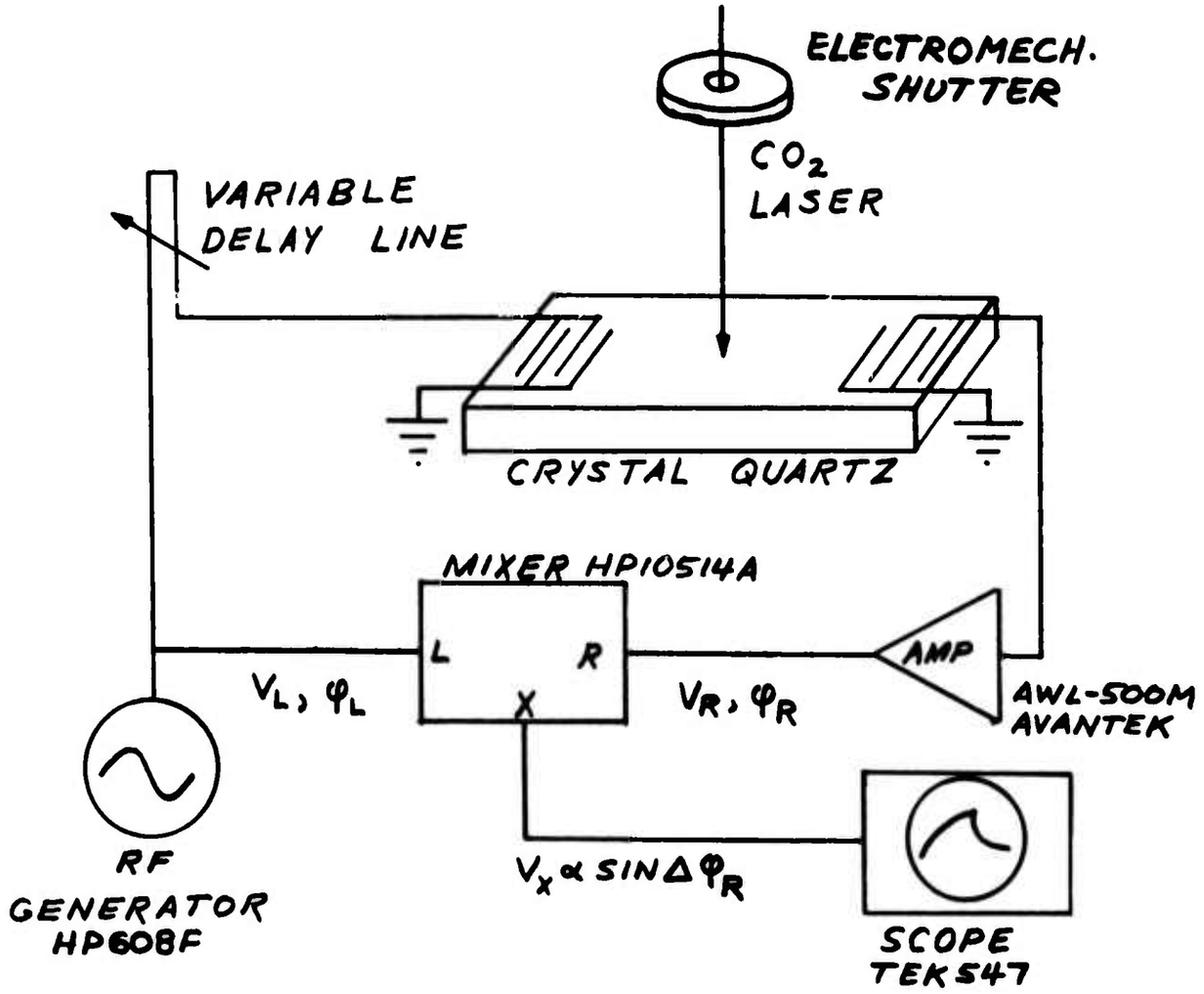

Figure 1 Experimental apparatus used to measure induced phase shifts.

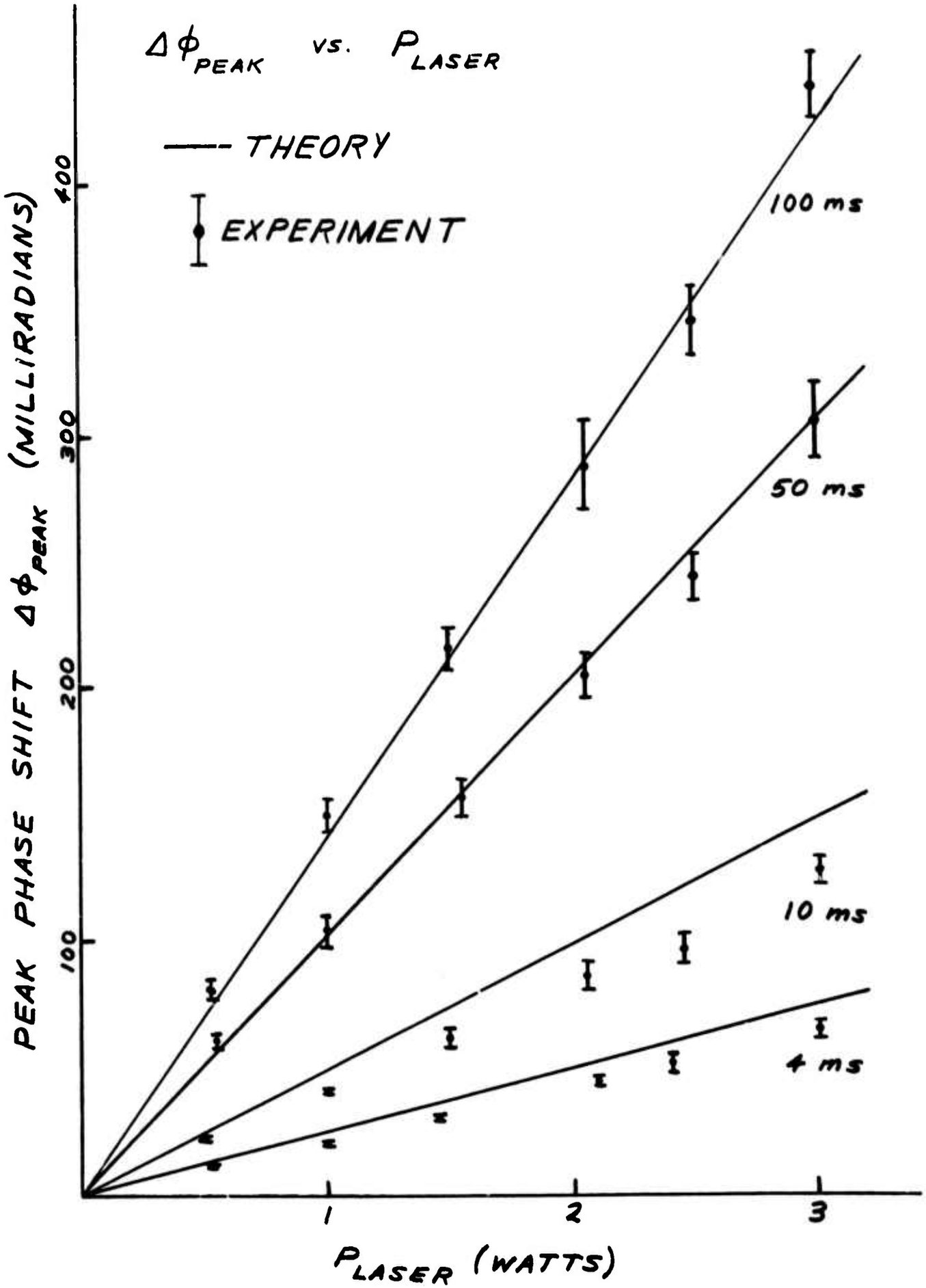
$\Delta\phi_{PEAK}$ vs. P_{LASER}
THEORY
EXPERIMENT
100 ms
50 ms
10 ms
4 ms
PEAK PHASE SHIFT $\Delta\phi_{PEAK}$ (MILLIRADIANS)
100
200
300
400
1
2
3
P_{LASER} (WATTS)

FIGURE 2

f.3 Absorption Studies of CdTe and ZnSe

W. G. Spitzer, B. V. Dutt

The initiation of a study of the infrared absorption of CdTe and ZnSe and the mechanisms responsible for the absorption is the subject of this progress report. The long range purposes of this investigation are to identify the absorption mechanisms and the spectral range in which they influence the optical properties. For this program it will be necessary to obtain material from a variety of sources including our own crystal growth efforts and to establish procedures for the introduction of controlled concentrations which are potentially identifiable. The measurements will include infrared transmission and reflection for a broad spectral region as well as calorimetric measurements near 10.6μm. Other measurements such as electron microscopy, ion microprobe, x-ray, etc. will be made as the experimental conditions indicate their desireability.

In this quarter we report the results of a literature survey, some initial attempts at CdTe crystal growth, and the preliminary absorption measurements of both heat treated and lithium-diffused material.

Literature Survey: A review of the literature on ZnSe and CdTe with respect to lattice absorption, free carrier absorption, and impurity absorption, and transport properties was undertaken. The conditions during growth and/or post growth annealing influence these properties because of the resulting changes in free carrier concentration and the change in concentration and character of the defect centers. Table I lists some of the properties of doped CdTe observed by various authors. Table 2 gives a short collection of some of the luminescence properties as well as localized vibrations of impurities studied in ZnSe.

Source of Material: We have obtained material from the following sources:

(1) our own crystal growth efforts yielded a boule of CdTe+Cr. The method of growth employed was the travelling heater method which is used to grow crystals under well-defined Te pressures.

(2) Hughes Research Center; CdTe undoped (courtesy of Dr. G. Picus).

(3) II-VI, Inc. Boules of large grain polycrystalline CdTe+In (In:5×10^{17}/cc) and CdTe+Cl (Cl: 5×10^{16}/cc) and two pieces of undoped polycrystalline ZnSe were purchased. The ZnSe was grown at Raytheon Corp.

(4) We just received some ZnSe and CdTe through the courtesy of Dr. D.C. Reynolds of the Aerospace Research Laboratories (AFSC), Air Force Base, Dayton.

Effects of Annealing: In an effort to evaluate and understand the effects of annealing on the absorption in CdTe and ZnSe (both doped and undoped), a first set of measurements were done with a conventional grating spectrometer in the

in the spectral range from 600 to 230cm^{-1}. CdTe was annealed under controlled Cd and Te-rich conditions. The primary annealing study was carried out on CdTe (Hughes) CdTe+Cl (II-VI, Inc.) and CdTe+In (II-VI, Inc.) in a two zone furnace with the crystal in the higher temperature zone, $T_{crystal}$ = 885°C, and with either Cd or Te at the lower temperature, T_{Cd} = 750°C, T_{Te_2} = 716°C. The latter temperatures correspond to $P_{Cd} \approx 1$ atm and $P_{Te_2} \approx 5.10^{-2}$ atm., respectively. The first observations indicate that the absorption level in the annealed crystals is higher than that in the untreated crystals with some differences which appear to depend upon the initial doping. The results are being analyzed to plan the next annealing procedures with a view to understand the absorption processes. Also similar preliminary annealing effect measurements on ZnSe are bein initiated. To study the effects of annealing and stoichiometry on the absorption at 10.6μm, we prepared a corresponding set of samples for calorimetric measurements which are now being made. The results will be given in the next report.

Impurity Absorption: The earlier studies[12, 14] of lithium doped CdTe and ZnSe show that there is increased absorption due to lithium. The localized vibrations resulting from the lithium centers are not well understood and may involve defect complexes. In both of the earlier studies, the lithium was introduced in the melt during growth of the crystals.

Experiments are underway to diffuse lithium (^{7}Li and ^{6}Li separately and also simultaneously) to study the defect complexes via localized mode vibrational studies along the lines indicated by Levy's work[13] on GaAs. This will be done for both CdTe and ZnSe.

Our preliminary absorption measurements on ^{7}Li-doped CdTe and ZnSe indicate complete opacity in the regions, where the local modes are reported in references 12 and 14. This may be due to the higher concentration of lithium in our samples.

Also, our preliminary diffusion anneals were carried out from an alloyed layer of ^{7}Li which was first applied in the form of a mineral oil suspension onto CdTe and ZnSe and then alloyed by heating to 800°C in Ar atm. The samples are damaged and become excessively brittle and therefore we plan to do the lithium diffusion from evaporated layers. An existing vacuum system with a heater to do these diffusion runs has been modified for this work and the first trials will be made shortly.

References

1. H. Kato and Takayanagi, Jap. J.A.P. 2 (1963), p. 250.
2. I. Teramoto and S. Takayanagi, J. Phys. Soc. (Japan), (1962), p. 1137
3. D. de Nobel, "Phase Equilibrium and Semiconducting Properties of CdTe", Thesis, University of Leiden, May 1958.
4. B. M. Vul, et al., Soc. Phys. (Semiconductors), V8 (1), p. 206, (1966)
5. V. V. Matlak, et al., ibid, pp. 1760-61.
6. G. H. Kachurin, et al., Sov. Phys. Rev. (Semiconductors) 2 (12), 1969, p. 1527
7. J. P. Donnelly et al., Appl. Phys. Lett., 12, (9), (1968), p. 303
8. U. V. Desmica & N. B. Urh, Phys. Rev (B), 6 (8), (1972), p. 3044.
9. E. N. Arkadeva, et. al., Sov. Phys. (Semiconductors), 2 (10), (1969), p. 1264
10. W. Haye and A. R. L. Spray, J. Phys. C., Sev. 2, Vol. 2 (1969), p. 1129
11. M. Aven and R. E. Haltsted, Phys. Rev., Vol. 137, A28, (1965)
12. A. Mitsuishi, et al., Suppl. of the Prog. of Theoretical Phys., No. 45, (1970), p. 21
13. M. E. Levy and W. G. Spitzer, J. Phys. C. Solid State Phys., Vol. 6, 1973 3223.
14. M. Balkanski, et al., Localized excitations in Solids, R. F. Wallis, p. 154

TABLE I: PROPERTIES OF CdTe WITH VARIOUS IMPURITIES

DOPANT	METHOD OF DOPING	PROPERTY MEASURED AND THE CONDITIONS OF MEASUREMENT	PROPOSED DEFECT MODEL	REMARKS	REFERENCES
In	Diffusion from vapor (450-1000°C)	Assuming const. surface concn. $D = 4.1.10^{-2} \exp\left[-\frac{37 \pm 3.5 \text{Kcal/mole}}{RT}\right]$ $= 4.1.10^{-2} \exp\left[-\frac{1.61 \pm 0.152 \text{eV}}{RT}\right]$	$In_{Cd}^{\cdot}$ (Single donor) Diffusion by vacancy mechanism on Cd sites charged state of diffusing species unknown.	No comments given about compensating species; nothing about levels.	(1) H. Kato & S.Takayanagi
In (5.10^{17}/cc)	Zone leveling	(1) Distribution coefft. K = Cs/Cl is $\simeq 0.5$ for In, Mg, Cu, Ag, Pb, and > 1 for Al. (2) In-doped samples show no p-type conductivity at all. At low P_{Cd} $\rho = 10^6$-$10^7 \Omega$cm. At high P_{Cd}, n-type going to higher P_{Cd}, $n \sim P_{Cd}^{1/2}$ and then $n \sim P_{Cd}^{o}$ and $= [In_{Cd}^{o}]$. (3) Photoluminescence at 77°K shows (900°C, P_{Cd} = 0.1 atm annealed) two peaks - large one at 1.42eV and a small one 1.10eV. (Annealing at P_{Cd} = 0.01 atm). Shows large peak at 1.42eV but a smaller peak at 1.06eV. (4) Photoconductivity shows peaks at 1.49 eV and a weak one at 1.07 eV. Annealing at P_{Cd} = 0.01 atm. shows 1.46 eV peak to be very large, but 1.07 eV was not found.	(1) High P_{Cd} $n \sim P_{Cd}^{o}$ and $n = [In_{Cd}^{\cdot}] = [In_{Cd}]_{tot.}$ (2) At lower P_{Cd} $n \sim P_{Cd}^{1/2}$ $2[V_{Cd}''] = [In_{Cd}^{\cdot}]$ $= [In_{Cd}]_{tot.}$ (3) At a certain P_{Cd}, n decreases suddenly, then very low $p = n + [V_{Cd}'] \longrightarrow$ $p = 2[V_{Cd}'']$		(3) D. de Nobel

TABLE I: PROPERTIES OF CdTe WITH VARIOUS IMPURITIES

DOPANT	METHOD OF DOPING	PROPERTY MEASURED AND THE CONDITIONS OF MEASUREMENT	PROPOSED DEFECT MODEL	REMARKS	REFERENCES
Au	Diffusion 600-1000°C in N_2 atm.	D = 67 exp (-2.0 eV/RT) dislocation density of samples $10^6/cm^2$/edge) determined by etch pit method. No pressure dependence work.	Au'_{Cd} = acceptor. Suggestion of compensation by holes. Diffusion by vacancy mechanism charged state unknown.	[h˙] measured by Hall measurements lower [h˙] at T < 400°C. Segregation and precipitation of Au at 60° α and β dislocations. This contradicts de Nobel's model that at T < 400°C Au, acts as a hole trap. Nothing about levels.	(2) I. Teramoto and S. Takayanagi

TABLE I: PROPERTIES OF CdTe WITH VARIOUS IMPURITIES

DOPANT	METHOD OF DOPING	PROPERTY MEASURED AND THE CONDITIONS OF MEASUREMENT	PROPOSED DEFECT MODEL	REMARKS	REFERENCES
Au	Zone levelling	1) Low P_{Cd}, P-type; at a certain P_{Cd} changes to n-type. 2) At 4.10^{16} Au/cc shows a range $[h^{\cdot}] \sim P_{Cd}^{o}$ 3) At 4.10^{17} Au, this range of independence of $[h^{\cdot}]$ on P_{Cd} was not found. 4) p to n-type changes for: 700°C; P_{Cd} = 0.4 atm. 800°C; P_{Cd} = 1.3 atm. 900°C; P_{Cd} = 3.2 atm. 5) Photoluminescence 15.10^{16} Au/cc annealed at 900°C, P_{Cd} = 0.2 atm. Immediately after preparation shows bands at 1.40 and 1.27 eV. Reheating for 1 hour at 100°C and cooling to ro room temperature decreases the intensity of the 1.27 eV peak. 6) Photoconduction (5.10^{16} Au/cc anneal at 900°C P_{Cd} = 0.2 atm) shows a peak at 1.60 eV and heating at 100°C markedly decreased the intensity.	$[h^{\cdot}] = [e']$ $[h^{\cdot}] = [Au'_{Cd}]$ $[h^{\cdot}] = [V'_{Cd}]$		(3) D. de Nobel

TABLE I: PROPERTIES OF CdTe WITH VARIOUS IMPURITIES

DOPANT	METHOD OF DOPING	PROPERTY MEASURED AND THE CONDITIONS OF MEASUREMENT	PROPOSED DEFECT MODEL	REMARKS	REFERENCES
Cu, Ag, Sb	Zone Levelling	1) Same behavior as in highly doped Au sample in the p-type region. 2) With CdTe + Ag or Cu, independent of the conditions of preparation only one peak at 1.40 eV was found. 3) Photoconductivity in Ag or Cu-doped samples shows a peak at 1.49eV 4) All the samples and very pure ones show the 1.49 eV peak.			(3) D. De Nobel
Fe	Diffusion at 900°C	$D_{(900°C)} = 4.10^{-8} cm^2/sec$. Two abs. bands seen at hV = 0.35 and 1.35 eV due to electron transitions within the iron center. Iron did not give any local levels in the bandgap.	Interstitial diffusion	ESR shows no Fe^{3+} state indirectly, indicating that Fe^{2+} is the species (Fe^{x}_{Cd}).	(4) B. M. Vul, et. al
Ge	Added to melt Bridgeman technique	p-type conduction. $\rho = 10^7$-$10^9 \Omega cm$. At higher T, some of the samples, with higher $\rho = 10^9 \Omega cm$ showed change of sign of Hall voltage.	Defects unidentified.		(5) V. V. Matlak, et. al.

TABLE I: PROPERTIES OF CdTe WITH VARIOUS IMPURITIES

DOPANT	METHOD OF DOPING	PROPERTY MEASURED AND THE CONDITIONS OF MEASUREMENT	PROPOSED DEFECT MODEL	REMARKS	REFERENCES
P	Diffusion at T ≯ 450°C in vacuum from the vapor phase.	P-type (low resistivity films)	$[h^{\cdot}]/Na = 1.15.10^{-3}$ low due to self-compensation effect.		(6) G. A. Kachurin et. al.
	Diffusion in sated Cd-vapor pressure	P-type			
	Ion implantation at Room temperature	The small ratio of $[h^{\cdot}]/Na$ was interpreted as due to the stopping of high proportion of phosphorus atoms in a disordered layer.		A reproducible phenomenon was observed. The resistance decreased with increasing dose only after a sample had been stored for a long time at room temperature Heating before bombardment made the films insensitive to irradiation. The effect is explained to be due to the interaction of p-atoms with some accidental impurity. This	

TABLE I: PROPERTIES OF CdTe WITH VARIOUS IMPURITIES

DOPANT	METHOD OF DOPING	PROPERTY MEASURED AND THE CONDITIONS OF MEASUREMENT	PROPOSED DEFECT MODEL	REMARKS	REFERENCES
P (Continued)				effect was not seen in CdTe films that were implanted by other ions.	
As	Ion implantation at 400 KeV	Started with n-type layer and p-n junction was produced.		Room temperature ion implantation introduced radiation damage, which does not anneal out in two days at 650°C and the layer was semi-insulating. Due to the high vapor pressure of CdTe, implantations were done at 500°C using SiO_2 encapsulated layers.	(7) J. P. Donnelly et.al.

TABLE I: PROPERTIES OF CdTe WITH VARIOUS IMPURITIES

DOPANT	METHOD OF DOPING	PROPERTY MEASURED AND THE CONDITIONS OF MEASUREMENT	PROPOSED DEFECT MODEL	REMARKS	REFERENCES
Li	Diffusion at 600, 680 and 750° C under corresponding P_{Cd} atm.	Resistivity and Hall measurements. p-type CdTe. Two levels at E_V + 0.14 eV and E_v + 0.27 eV.	Amphoteric behavior of lithium was proposed (Li'_{Cd} and Li_i species).	Possible model $[h^\cdot] + [li_i] = [Li'_{Cd}]$ Complexes involving Li and Cd vacancies are also a possibility $(Li_{Cd}Li_i)^x$ Mobility increases at lower temperatures.	(8) U. V. DeSnica and N. B. Urli
	Diffusion of Li into CdTe of n and p-type from a layer of Li in Ar atmosphere at T_D = 500°C		Diffusion by interstitial mechanism but occupies both Cd and interstitial sites.		(9) E. N. Arkad'eva et al.
Li	Added to melt in Bridgemann method	Localized vibrations at ∿ 270cm^{-1}	Centers inconclusive		(14) Balkanski, et al.

TABLE I: PROPERTIES OF CdTe WITH VARIOUS IMPURITIES

DOPANT	METHOD OF DOPING	PROPERTY MEASURED AND THE CONDITIONS OF MEASUREMENT	PROPOSED DEFECT MODEL	REMARKS	REFERENCES
Be	Bridgemann method	IR absorption of Be:CdTe in the range 1-1000μ	Be_{Cd}: Substitutional Be on Cd sites charged rate	Fundamental of local vibrational mode at 391cm^{-1} (4°K) one second harmonic and two third harmonics are also found.	(10)

TABLE II: ZnSe: Luminescence and Localized Vibrations Due to Impurity Centers.

DOPANT	METHOD OF DOPING	PROPERTY MEASURED & THE CONDITIONS	PROPOSED DEFECT MODEL	REFERENCE
Cu	Diffusion (300 570°C) in H_2 atm at 1 atm. $D = 55.10^{-9} cm^2/sec$ at 510°C or $D = 1.7.10^{-5} \exp(-0.56eV/RT)$	Luminescence: Green at 2.36 eV	Cu'_{Zn} (acceptor)	Aven and Halsted (11)
ZnSe: Cl_n ($Cu.diff^n$)	"	"	"	"
ZnSe:Al ($Cu.diff^n$)	$2.6.10^{-11}$ reduced by a	Luminescence	$(V''_{Zn} Al^{\cdot}_{Zn}) = (V_{Zn}Al_{Zn})'$ The reduced $diff^n$ may be due to Cu^x_{Zn} + $(V''_{Zn}Al^{\cdot}_{Zn}) = [(Cu'_{Zn}Al^{\cdot}_{Zn})]$ Converting the yellow luminescence of $(V_{Zn}Al_{Zn})'$ at 2.07eV to red luminescence at 1.95eV $Diff^n$ is via interstitial with interstitial substitutional equilibrium.	

TABLE II: ZnSe: Luminescence and Localized Vibrations Due to Impurity Centers

DOPANT	METHOD OF DOPING	PROPERTY MEASURED & THE CONDITIONS	PROPOSED DEFECT MODEL	REFERENCE
Al	Added in melt	Local modes $359cm^{-1}$	Al'_{Zn} There are two groups on either side. At the highest concentration (1.8×10^{20}/cc) new bands are observed at 364, 354 and 325 cm^{-1} due to unresolved complexes	A. Mitsuishi, et. al (12)
^{6}Li	"	$412cm^{-1}$		
^{7}Li	"	$383cm^{-1}$		
Be	"	$450cm^{-1}$		
^{24}Mg	"	$352cm^{-1}$		
^{25}Mg	"	$345cm^{-1}$		

g.1 Characterization of Optical Performance of IR Window Systems

J. H. Marburger

During this quarter the thermal lensing formalism described in detail in the previous report was developed further and applied to windows with residual birefringence not induced by thermal absorption. A detailed account will be reported in the next quarterly report, but a brief sketch is provided below. We have also computed the relative contributions of the elementary fields E_o and E_2 described in the previous report (Equations (5.5) and (5.6) for typical window models. Our results are now being analyzed and will be included in the continuation of our narrative review begun in the previous report and to be continued in the next quarterly report. Preliminary analysis indicates that the effects of birefringence are negligible. That is, the dependence of the refractive index upon stress makes itself felt much more strongly through the mean index change than through induced birefringence. This allows a vast simplification in the approximate analysis of focal intensity degradation in systems with large stress-optic coefficients.

The analysis of residual birefringence is most easily approached through the aberration matrix formalism outlined in the previous report. Thus the exit field $\vec{E}(\vec{r}, o)$ is related to the entrance field into the window $\vec{E}(\vec{r}, -w)$, by

$$\vec{E}(\vec{r}, o) = \vec{\vec{A}}(\vec{r}) \cdot \vec{E}(\vec{r}, -w),$$

where the aberration matrix is

$$\vec{\vec{A}}(\vec{r}) \equiv \exp i\left[2\pi k_1 w \vec{\vec{\chi}}(\vec{r}) / n_1^2\right].$$

Here n_1, k_1 are the window index and optical wave numbers and w is the window thickness, all evaluated at zero incident field. All induced changes in dielectric tensor or path length through the window are included in $\vec{\vec{\chi}}$. In our previous work, we analyzed the properties of $\vec{\vec{A}}$ when the local principal axes of $\vec{\vec{\chi}}$ and $\vec{\vec{A}}$ were parallel to local polar coordinates (axial symmetry). If the medium has additional anisotropy of different symmetry, we can isolate it in a separate term in $\vec{\vec{\chi}}$:

$$\vec{\vec{\chi}} = \vec{\vec{\chi}}_o + \vec{\vec{\chi}}_i$$

where $\vec{\vec{\chi}}_o$ is the intrinsic susceptibility tensor, and $\vec{\vec{\chi}}_i$ the additional contribution from thermally induced effects.

Thus the aberration matrix is

$$\vec{\vec{A}} = \exp\left[i (2\pi k_1 w / n_1^2) \cdot (\vec{\vec{\chi}}_o + \vec{\vec{\chi}}_1) \right] , \qquad (1)$$

which can be factored if $\vec{\vec{\chi}}_o$ commutes with $\vec{\vec{\chi}}_1$:

$$\vec{\vec{A}} = \vec{\vec{A}}_o \cdot \vec{\vec{A}}_1 ,$$

but in general cannot be further reduced except in special cases.

In the particular case of uniform background birefringence, with principal axes of $\vec{\vec{\chi}}_o$ along x and y, we have

$$\vec{\vec{\chi}}_o = \chi_x \, \hat{x}\hat{x} + \chi_y \, \hat{y}\hat{y} ,$$

and the aberration matrix including induced birefringence for a circular beam is

$$\vec{\vec{A}} = e^{i\varphi} \begin{bmatrix} \cos\Theta + \sin\Theta\,(\zeta + \Delta\cos 2\theta) & \Delta \sin 2\theta \\ \Delta \sin 2\theta & \cos\Theta - \sin\Theta\,(\zeta + \Delta\cos 2\theta) \end{bmatrix} \qquad (2)$$

Here φ is the mean phase increment in the window (proportional to $\frac{1}{2}$ Tr $(\vec{\vec{\chi}}_o + \vec{\vec{\chi}}_1)$, and ζ is half the difference in phase increment for $\hat{x}$ and $\hat{y}$ polarized light without induced birefringence. Δ and θ are the same as the variables appearing in eq. (4.6) in the previous report, and

$$\Theta^2 = \Delta^2 + \zeta^2 + 2\,\zeta\,\Delta\cos 2\theta \quad . \qquad (3)$$

In the absence of the background birefringence, the θ dependent term in (3) is absent (because $\zeta = 0$) and the angular part of the diffraction integral which gives the focal properties of the exit field can be performed easily. Our approach is to expand the aberration matrix in powers of $\cos 2\theta$ and $\sin 2\theta$, and keep only the first few terms. This is a good approximation, because each higher term leads to a bessel function of higher order in the argument of the diffraction integral, and these do not influence the axial intensity. Associated with each bessel function is a correction to the polarization of the exit field.

h.1 Initial Investigation of the Role of Inclusion Damage in the Failure of 10.6μm Optics

M. Bass, L.G. DeShazer and K.M. Leung

During this quarter, work was directed toward the construction of a CO_2 TEA laser. This laser, when completed, will deliver ~100 mJ of TEM_{00} mode output at 10.6μm. Four major tasks were undertaken towards the completion of this laser.

h.1.a Acquisition of Parts, Components, and Supporting Equipment

All necessary parts and components for the discharge circuit, trigger/heater unit, and gas handling system were obtained. The order for the high-voltage power supply had been held up due to a funding mix up. This has been corrected and the unit ordered. Delivery is to be on 4/19/74. Fortunately, we were able to borrow a supply from another group to use temporarily.

h.1.b Machine Work

The resonator box, platform, and laser cabinet were made by the USC Engineering Machine Shop. The construction has been completed.

h.1.c Installation of New Facilities in the Laboratory

New facilities such as an electrical ground, optical tables, and gas cylinder holding rack were installed in the laboratory to support TEA laser operation. Only the exhaust system for the laser remains to be installed.

h.1.d Construction of the CO_2 TEA Laser

The laser resonator is a large plexiglas box which contains the major parts of the discharge circuit including two Rogowski electrodes, the spark gap, and the energy storage capacitors. With the KCl Brewster windows attached to both sides of the resonator, it acts like a pressure-tight box. The window heater was immediately activated to warm the slightly hygroscopic KCl windows. The external trigger unit controls the firing of the laser. The gas handling system can handle the mixing of four different gases. For the TEA laser, only three gases - N_2, CO_2 and He, are used.

We have assembled this laser system and started initial testing. No serious arcing problem was encountered when firing the laser. However, arcing between the upper trigger wire and one of the electrodes has prevented the uniform breakdown of the main discharge. We are in the process of trouble shooting this problem. As soon as the laser's performance is optimized, we shall identify the various beam parameters on the device. A photon-drag detector is being constructed for monitoring the laser pulse waveform.

In addition to the construction of the TEA laser, we have acquired seventeen samples of ZnSe and KCl materials. Two samples of ZnSe were grown by Raytheon. One sample is on loan from Wright-Patterson Air Force Base. For KCl single crystals, five samples were furnished by Harshaw and nine samples by International Crystal Laboratory. One KCl sample is also on loan from Wright-Patterson Air Force Base.

In the following quarter, we shall first characterize these samples by optical microscopy and calorimetry, and then begin our measurements on damage threshold of these samples to determine the influence of inclusion damage at 10.6μm.

3. DISCUSSION

Measurement of the IR absorption of another sample of melt grown GaAs again showed the same spectrum with broad peaks at 9.7 and 10.65μm in approximately the same intensity. Whereas heating in oxygen at 400°C caused some increase in the absorption, heating at the same temperature in vacuum did not produce a change. The previous increase in either due to oxygen or to contamination with copper or iron from the furnace wall; annealing of the contaminated sample at 1100°C produced some further increase of absorption.

The two-peak absorption is probably intrinsic and due to multiphonon absorption. The observed wavelength variation supports this view. If this is correct, the absorption observed cannot further be diminished.

Good progress is being made with the construction of apparatus for the growth of thick epitaxial layers of GaAs from liquid gallium, which will enable us to give a final verdict on GaAs.

Studies of the mechanical behavior of GaAs gives further evidence for the importance of Si_{Ga}-V_{Ga} pairs as the cause of observed dynamic hardening. The yield stress increases under the same conditions under which local mode studies show the increased formation of Si-V pairs.

Work on the removal of oxygen from liquid gallium by electro-chemical pumping with the aid of a zirconia solid electrolyte cell, and the measurement of the residual oxygen content of the melts with the same cell, shows continuing promise for this technique. However, the work is hindered by frequent cracking and breakage of the zirconia ceramics. Methods of usage that prevent cracking as far as possible have been developed.

Work on CdTe, carried out with CdTe doped with 5×10^{16} Cl, has shown carrier concentrations as $f(P_{Cd},T)$ as expected for such a weakly doped material. Annealing at 700, 800, 900°C at various cadmium pressures followed by rapid cooling shows a sharp minimum of both the carrier concentrations and the absorption coefficient at 10.6μm at the expected point.

The lowest carrier concentrations and absorption are found for annealing at 700°C, with $k_{10.6\mu} = 3 \times 10^{-3}cm^{-1}$. The absorption varies linearly with the hole concentration, showing that the absorption is due almost entirely to free carriers.

Measurements of the dielectric constant of insulating CdTe are in progress. The capacitance was found to be independent of the electric field and frequency from $1\text{-}10^4$V/cm and 10kHz to 1MHz. Hotpressing of CdTe with the aid of liquid Cd or Te as volatile sintering aids are hindered by unsatisfactory wetting of

of the CdTe by these agents.

The alkali halide work was concentrated on KBr. Impurities must be responsible for the residual absorption in excess of the expected multiphonon absorption. Crystals were prepared with various dopants; only bromate ions caused a markedly increased 10.6 μm absorption, suggesting that bromate may be the active impurity in our purest crystals. Attempts to remove it from molten KBr by reduction with CBr_4 failed due to excessive carbonization.

Improvements in the crystal growing furnace will make possible the growth of faceted KBr crystals.

A CO_2 TEA laser for damage has been assembled and is presently being tested.

The theoretical group developed an accurate expression for the non-linear moment contribution to the multiphonon absorption of crystals with NaCl structure. The expression was applied to a lattice model with nearest neighbor springs. The improved model yields difference as well as summation bands.

The theory of thermal lensing was extended to include residual birefringence. It was found that the effect of the latter is negligible.

For the acoustic probe studies of surface properties using surface waves, a theory for the interaction of surface waves with a surface heated by strongly absorbed radiation was developed. It was found to represent results for radiation with a 10.6μm laser with a pulse width $\tau_p \leq$ 10msec with a systematic one-sided discrepancy of 15% for greater pulse lengths the discrepancy was reduced to 5%.